New Phytologist

Research

Flexure wood formation via growth reprogramming in hybrid aspen involves jasmonates and polyamines and transcriptional changes resembling tension wood development

János Urbancsok[1]*, Evgeniy N. Donev[1]*, Pramod Sivan[1], Elena van Zalen[2], Félix R. Barbut[1], Marta Derba-Maceluch[1], Jan Šimura[1], Zakiya Yassin[3], Madhavi L. Gandla[4], Michal Karady[5], Karin Ljung[1], Sandra Winestrand[4], Leif J. Jönsson[4], Gerhard Scheepers[3], Nicolas Delhomme[1], Nathaniel R. Street[2,6] and Ewa J. Mellerowicz[1]

[1]Umeå Plant Science Centre (UPSC), Department of Forest Genetics and Plant Physiology, Swedish University of Agricultural Sciences, 90183, Umeå, Sweden; [2]Umeå Plant Science Centre (UPSC), Department of Plant Physiology, Umeå University, 90187, Umeå, Sweden; [3]RISE Research Institutes of Sweden, Drottning Kristinas väg 61, 11428, Stockholm, Sweden; [4]Department of Chemistry, Umeå University, 90187, Umeå, Sweden; [5]Laboratory of Growth Regulators, Institute of Experimental Botany of the Czech Academy of Sciences and Faculty of Science of Palacký University, 78371, Olomouc, Czech Republic; [6]SciLifeLab, Umeå University, 90187, Umeå, Sweden

Author for correspondence:
Ewa J. Mellerowicz
Email: ewa.mellerowicz@slu.se

Received: *11 July 2023*
Accepted: *19 September 2023*

New Phytologist (2023)
doi: 10.1111/nph.19307

Key words: flexure wood, jasmonic acid signaling, mechanostimulation, polyamines, *Populus tremula* × *tremuloides*, saccharification, thigmomorphogenesis, wood development.

Summary

- Stem bending in trees induces flexure wood but its properties and development are poorly understood. Here, we investigated the effects of low-intensity multidirectional stem flexing on growth and wood properties of hybrid aspen, and on its transcriptomic and hormonal responses.
- Glasshouse-grown trees were either kept stationary or subjected to several daily shakes for 5 wk, after which the transcriptomes and hormones were analyzed in the cambial region and developing wood tissues, and the wood properties were analyzed by physical, chemical and microscopy techniques.
- Shaking increased primary and secondary growth and altered wood differentiation by stimulating gelatinous-fiber formation, reducing secondary wall thickness, changing matrix polysaccharides and increasing cellulose, G- and H-lignin contents, cell wall porosity and saccharification yields. Wood-forming tissues exhibited elevated jasmonate, polyamine, ethylene and brassinosteroids and reduced abscisic acid and gibberellin signaling. Transcriptional responses resembled those during tension wood formation but not opposite wood formation and revealed several thigmomorphogenesis-related genes as well as novel gene networks including *FLA* and *XTH* genes encoding plasma membrane-bound proteins.
- Low-intensity stem flexing stimulates growth and induces wood having improved biorefinery properties through molecular and hormonal pathways similar to thigmomorphogenesis in herbaceous plants and largely overlapping with the tension wood program of hardwoods.

Introduction

The ever-changing environment represents a constant challenge to all living organisms, hence proper perception and response to diverse external stimuli is crucial for their survival. These abilities are particularly important for sessile organisms such as plants. Plants evolved in environments rich in diverse mechanical stimuli whose perception and subsequent adjustment of growth and development is called thigmomorphogenesis (Jaffe, 1973; Chehab *et al.*, 2009; Telewski, 2021; Brenya *et al.*, 2022). It involves growth redistribution resulting in more compact form and expanded root system (Jaffe, 1973; Telewski & Jaffe, 1986a,b; Braam & Davis, 1990; Gartner, 1994; Telewski & Pruyn, 1998; Pruyn *et al.*, 2000; Braam, 2005; Kern *et al.*, 2005; Coutand *et al.*, 2008; Coutand, 2010; Wu *et al.*, 2016). It can also delay vegetative to reproductive phase transition (Chehab *et al.*, 2012). Mild mechanostimulation has been shown to increase the growth and resilience of plants to various abiotic/biotic factors in different crops, hence it has been proposed as a potential sustainable agricultural practice (Ghosh *et al.*, 2021).

Mechanostimulated plants also modify cell walls, as evidenced by upregulation of xyloglucan-, cellulose- and lignin-related genes, and genes encoding fasciclin-like arabinogalactan proteins (FLAs) in *Arabidopsis thaliana* (Xu *et al.*, 1995, 2019; Lee *et al.*, 2005; Saidi *et al.*, 2010). Trees exposed to mechanical disturbance develop a special kind of wood, called flexure wood

*These authors contributed equally to this work.

© 2023 The Authors
New Phytologist © 2023 New Phytologist Foundation
This is an open access article under the terms of the Creative Commons Attribution-NonCommercial License, which permits use, distribution and reproduction in any medium, provided the original work is properly cited and is not used for commercial purposes.

(Telewski, 1989, 2016). Development of flexure wood involves increased radial growth, especially in the direction of mechanical stress, which can lead to stem ovality, thickened cell walls, increased cellulose microfibril angle (MFA), reduced diameter and length of tracheary elements, and in the case of angiosperms, reduced frequency of vessel elements relative to fibers compared with normal wood. Xyloglucan deposition was recorded in the wood formed during seismic activity in hardwoods (Kaida *et al.*, 2020). Flexure wood increases mechanical resilience of hardwood and softwood trees (Telewski & Jaffe, 1986b; Niez *et al.*, 2020), which could impact timber quality for solid wood products. However, its effect on wood biorefinery-related properties has not been investigated.

In addition to flexure wood, woody plants can develop reaction wood (tension wood in case of hardwoods or compression wood in case of softwoods) to gravitropically bend secondarily thickened stems (Groover, 2016). The structure and composition of cell walls in tension and compression wood are modified. Tension wood fibers in many hardwoods reduce deposition of secondary wall layers and instead produce a thick, unlignified tertiary cell wall layer called gelatinous layer, which contains high amounts of axially oriented cellulose, and low amounts of matrix polysaccharides, primarily β-1,4,-galactan. By contrast, the compression wood tracheids of softwoods modify their S2 layer by producing helically oriented cellulose and increasing lignification, and by adding an inner S2 layer with helical thickenings that contain β-1,4,-galactan and deposit callose between the thickenings. These modifications of tension and compression wood induce longitudinal tension and compression in the wood, respectively, driving stem bending.

The mechanisms of mechanoperception and subsequent growth reprogramming are complex and poorly understood (Telewski, 2021; Brenya *et al.*, 2022). Mechanoresponses are triggered within seconds and involve the cell wall, plasma membrane, cytosol and mitochondria (Baluška *et al.*, 2003; Xu *et al.*, 2019), followed by systemic reaction (Toyota *et al.*, 2018) and changes in chromatin responsible for stress acclimation (Coutand, 2010). Structural changes in the cell wall and plasma membrane are thought to activate different mechanosensitive ion channels responsible for converting the mechanical cues to essential ion fluxes, in particular Ca^{2+} (Nakagawa *et al.*, 2007; Monshausen & Haswell, 2013; Basu & Haswell, 2017) and plasma membrane-localized receptor-like kinases that transduce signals via mitogen-activated protein (MAP) kinase cascades and other protein phosphorylation relays (Wang *et al.*, 2018a). The elevated intracellular Ca^{2+} concentration is sensed mainly by calmodulin and calmodulin-like (CML) proteins, mRNAs of which are highly represented among the early touch-response transcripts (Braam & Davis, 1990; Lee *et al.*, 2005). Ca^{2+} signaling was reported to induce production of reactive oxygen species (ROS; Benikhlef *et al.*, 2013), and these pathways possibly overlap with cell wall integrity maintenance mechanisms (Bacete & Hamann, 2020). Downstream signals involve the crosstalk of jasmonates and gibberellins (GAs; Brenya *et al.*, 2020, 2022), when jasmonic acid (JA) via MYC2/3/4 (Chehab *et al.*, 2012; Van Moerkercke *et al.*, 2019) and GA catabolism mediated by gibberellin 2-oxidases (Lange & Lange, 2015) are responsible for inhibition of stem elongation.

Even though a growing body of evidence indicates that mechanical stimuli can alter tree growth and induce flexure wood formation, there are few detailed descriptions of the properties of flexure wood and tree trunk thigmomorphogenesis, especially for hardwood species (Telewski, 2016). Moreover, the hormonal responses to stem bending and the molecular mechanisms of mechanoperception and signal transduction events that lead to flexure wood formation are poorly understood, although a pioneering transcriptome analysis following single stem bending (Pomiès *et al.*, 2017) suggested some similarities with the general thigmomorphogenesis program in herbaceous plants. An early woody stem thigmomorphogenesis marker was identified as a Cys2/His2-type zinc finger transcription factor (TF) ZFP2 (Leblanc-Fournier *et al.*, 2008; Martin *et al.*, 2009, 2014), which is induced within minutes by a single stem bending (Coutand *et al.*, 2009) and could be involved in suppressing mechanoresponses as part of the de-sensitizing mechanism (Martin *et al.*, 2014). In the current study, we characterized hybrid aspen (*Populus tremula* L. × *tremuloides* Michx.) growth responses to repeated low-intensity multidirectional flexures, especially their effects in developing wood, including changes in wood structure, chemistry, transcriptome and hormonal profiles. We also tested whether flexure wood has improved saccharification properties.

Materials and Methods

Plant material and growth conditions

Hybrid aspen (*Populus tremula* L. × *tremuloides* Michx., clone T89) was micropropagated *in vitro*, transferred to soil and grown in the glasshouse as described in detail in Supporting Information Methods S1. For the first 2 wk, all trees were grown under stationary conditions. From the third week, a set of 13 trees (flexure set) were subjected to two series of *c.* 50–60 sudden accelerations and stops per day with pot rotations on a conveyor belt resulting in stem swaying movements (Video S1). The ultimate speed of the belt was $0.2\ m\ s^{-1}$, and it was reached in at most 1.5 s as could be seen on the video, which would result in acceleration of at least $0.13\ m\ s^{-2}$. The maximum angle from the vertical recorded with a digital camera at two consecutive stops for nine trees was $3.7° \pm 0.12$ (SE). The accelerations and stops also caused vibration of the stems. The other set of 13 trees were kept on the immobile belt (stationary set) throughout the growth period.

Assessment of growth

Stem height and diameter at the stem base were measured with a measuring tape and caliper, respectively. The aboveground biomass was recorded by weighing freshly cut shoots. Developing leaves, starting from leaf 8 (which was the first unfolded leaf from the apex) and ending at leaf 22, were collected and digitalized using a scanner followed by the calculation of their leaf area by ImageJ (Schneider *et al.*, 2012). The average internode length

© 2023 The Authors
New Phytologist © 2023 New Phytologist Foundation

14698137, 0, Downloaded from https://nph.onlinelibrary.wiley.com/doi/10.1111/nph.19307 by Swedish University Of Agricultural Sciences, Wiley Online Library on [15/11/2023]. See the Terms and Conditions (https://onlinelibrary.wiley.com/terms-and-conditions) on Wiley Online Library for rules of use; OA articles are governed by the applicable Creative Commons License

was determined for internodes 35–55. Belowground biomass was determined by weighing cleaned and air-dried roots.

Wood microscopy analysis

Wood samples of internodes 36–37 were fixed in FAA (4% formaldehyde, 5% acetic acid and 50% ethanol). Transverse 40–50 µm-thick sections were prepared with a vibratome (VT1000S; Leica Biosystems, Nussloch, Germany) and stained with a solution of one volume of 1% (w/v) Safranin O (CAS 477-73-6; Sigma-Aldrich) in 50% ethanol and two volumes of 1% aqueous (w/v) Alcian Blue (CAS 123439-83-8; Sigma-Aldrich). Images were acquired using a Leica DMi8 microscope (Leica Biosystems) and analyzed with ImageJ. Tension wood was identified by the presence of gelatinous fibers (G-fibers).

Cell wall chemical analyses

Forty centimeter-long stem segments below internode 37 from seven trees per set were debarked and freeze-dried for 48 h. Wood powder from individual trees for Py-GC/MS and trimethylsilyl (TMS) analyses was obtained with a file and sieved with Retsch AS 200 analytical sieve shaker (Retsch GmbH, Haan, Germany) to isolate 50–100 µm-particles. Fifty micrograms (±10 µg) of this powder was pyrolyzed in a pyrolyser equipped with an autosampler (PY-2020iD and AS-1020E; Frontier Lab, Koriyama, Japan) connected to a GC/MS (7890A/5975C; Agilent Technologies Inc., Santa Clara, CA, USA) and analyzed according to Gerber *et al.* (2012). Alcohol-insoluble residue (AIR) was generated as described by Gandla *et al.* (2015) and enzymatically destarched as described by Pramod *et al.* (2021). Portions of 500 µg (±10%) of destarched AIR were acid-methanolyzed and derivatized by TMS procedure; then, the silylated monosaccharides were separated by GC/MS (7890A/5975C; Agilent Technologies Inc.) according to Gandla *et al.* (2015). Raw data MS files were converted to CDF format in Agilent Chemstation Data Analysis (v.E.02.00.493) and processed in R (v.4.1.3; R Core Team, 2022) for peak identification. 4-*O*-methylglucuronic acid was identified according to Chong *et al.* (2013). Destarched AIR of seven trees per set was pooled and five portions of 3 mg were used for cellulose analysis by the Updegraff method (Updegraff, 1969), followed by glucose content determination with the anthrone method (Scott & Melvin, 1953).

Saccharification assay and nanoporosity analysis

Freeze-dried stem segments of seven trees per set had their pith removed and were ground using Retsch Ultra Centrifugal Mill ZM 200 (Retsch GmbH) equipped with a 0.5 mm ring sieve and sieved with a Retsch AS 200 vibratory sieve shaker to obtain particle size of 100–500 µm. Analytical-scale saccharification (Gandla *et al.*, 2021) was performed using five portions, each consisting of 50 mg of dry material pooled from seven trees per set, either pretreated in 1% (w/w) sulfuric acid (based on mass of reaction mixture) at 165°C for 10 min in an initiator single-mode microwave instrument (Biotage Sweden AB, Uppsala, Sweden) followed by enzymatic hydrolysis or used directly for the enzymatic hydrolysis at 45°C using 4 mg of the liquid enzyme mixture Cellic CTec2 (cat. nr. SAE0020; Sigma-Aldrich). Samples were analyzed for Glc production rate at 2 h by using an Accu-Chek® Aviva glucometer (Roche Diagnostics Scandinavia AB, Solna, Sweden). After 72 h of incubation, the yield of monosaccharides (Ara, Gal, Glc, Xyl and Man) was determined using a high-performance anion-exchange chromatography (HPAEC) system with pulsed amperometric detection method (Ion Chromatography System ICS-5000 by Dionex, Sunnyvale, CA, USA; Wang *et al.*, 2018b).

The surface area of wood powder was analyzed by using the Brunauer–Emmett–Teller (BET) method (Brunauer *et al.*, 1938) in a single-point BET automated gas adsorption analyzer (Tristar 3000 BET analyzer by Micromeritics, Norcross, GA, USA) using five technical replicates of pooled material (particle size of 100–500 µm) from seven trees per set. Nonspecific adsorbents were removed from samples by a 3 h degassing procedure using a SmartPrep Degasser (Micromeritics) before analysis.

SilviScan analysis

A SilviScan instrument (RISE, Stockholm, Sweden) was used for determining wood and fiber properties at the base of the stem for seven trees per set. Radial bark-to-bark stem sections having 2 mm tangential width and 7 mm height were prepared and equilibrated at 23°C and 43% relative humidity before the measurements. Wood density along the radius was determined using X-ray transmission whereas MFA was estimated by X-ray diffraction (Evans *et al.*, 1996; Evans & Ilic, 2001). The average density of each section was determined by measuring its volume and weight.

RNA extraction and transcriptomics

Developing xylem and cambium tissues were scrapped from the frozen debarked wood surface or from the inner surface of the corresponding bark, respectively, of *c.* 30 cm-long stem segments above internode 35. Total RNA was isolated according to Chang *et al.* (1993) and was subsequently purified using an RNeasy Plant Mini Kit (Qiagen GmbH, Hilden, Germany). RNA quantity and quality were determined by NanoDrop 2000 (Thermo Fisher Scientific, Waltham, MA, USA) and Agilent 2100 Bioanalyzer (Agilent Technologies Inc.), respectively. cDNA libraries were prepared and sequenced using NovaSeq 6000 PE150 at Novogene Co., Ltd (Cambridge, UK). Raw sequence data preprocessing and quality assessment are described in Methods S1. The reads were aligned to the *P. tremula* genome assembly (v.2.2) retrieved from the PlantGenIE (https://plantgenie.org; Sundell *et al.*, 2015). Putative orthologs in *Populus trichocarpa* (v.3.1) and *Arabidopsis thaliana* (v.11.0) were retrieved from PlantGenIE or, for selected gene families, were determined by phylogenetic analyses at PlantGenIE. Gene Ontology (GO) enrichment analysis, co-expression networks and heatmaps were obtained using PlantGenIE tools. The networks

© 2023 The Authors
New Phytologist © 2023 New Phytologist Foundation

14698137, 0, Downloaded from https://nph.onlinelibrary.wiley.com/doi/10.1111/nph.19307 by Swedish University Of Agricultural Sciences, Wiley Online Library on [15/11/2023]. See the Terms and Conditions (https://onlinelibrary.wiley.com/terms-and-conditions) on Wiley Online Library for rules of use; OA articles are governed by the applicable Creative Commons License

were visualized by CYTOSCAPE (v.3.6.0, Shannon *et al.*, 2003) and the heatmaps with COMPLEXHEATMAP (Gu *et al.*, 2016).

Hormone analyses

Cambium and developing xylem tissues (the same as used for RNA analyses) were subjected to hormone profiling using methods described by Šimura *et al.* (2018), with modifications described in Methods S1.

ACC quantification was performed in multiple reaction monitoring (MRM) mode employing an LC–MS/MS 1260 Infinity II LC System with Kinetex Polar C18 column (150 × 2.1 mm, 2.6 µm; Phenomenex Inc., Torrance, CA, USA) coupled to a 6495 Triple Quad LC/MS System with a Jet Stream and Dual Ion Funnel technologies (Agilent Technologies Inc.).

Polyamines (PAs) were extracted with methanol: chloroform: water (60 : 20 : 20; v/v/v), derivatized by AccQ-Tag™ (Waters, Milford, MA, USA) and analyzed by LC-ESI-MS/MS as described in Methods S1.

Results

Enhanced tree growth and altered stem anatomy in response to low-intensity flexure

The trees exposed to low-intensity stem flexures grew faster than trees maintained in stationary conditions (Figs 1a–g, S1). After five and a half weeks of flexure treatment, stem height and diameter were increased by 10%, internode length by 9%, aboveground biomass by 20%, root biomass by 24% and mature leaf size (leaf 22) by 32% compared with the control trees.

The nature of the increase in stem diameter of the flexure trees was further investigated by microscopy analysis (Fig. 2a–e). This revealed a 35% increment in wood area and a 43% decrease in pith area but no change in bark thickness, demonstrating that trees exposed to flexure produced more secondary xylem. Even though all trees, regardless of the presence of mechanical stimulus, developed tension wood characterized by the presence of G-fibers, exposure to regular flexure almost doubled the proportion of tension wood area relative to the total wood area.

Further assessment revealed differences in fiber cell walls when the two growth conditions were compared (Fig. 2f,g). In G-fibers, no change was observed for the thickness of the G-layer; however, the thickness of lignified cell wall layers (LL in Fig. 2g), including secondary cell wall and a half of the compound middle lamella, was *c.* 35% reduced in flexed compared with stationary trees. A similar reduction in thickness of lignified wall layers was observed in normal wood fibers. These data indicate that the flexure treatment stimulated secondary xylem formation, promoted G-fiber fate and inhibited secondary cell wall formation in both normal wood fibers and G-fibers.

SilviScan analysis (Fig. 2h–m; Table S1) showed that radial and tangential fiber diameters remained unaffected by flexure treatments, and that diameters of vessels or the frequency of vessels did not change significantly when comparing the two growth conditions. However, a 19% increase in the number of xylem cells produced by one fusiform initial was recorded in trees exposed to mechanical stimulation, providing evidence that the wider stem diameters and the larger total xylem areas of flexure-treated stems were caused by an increased rate of xylem cell production by the vascular cambium. Furthermore, SilviScan analysis revealed an increase in wood density and decrease in MFA, and consequently, the estimated modulus of elasticity (MOE), and fiber coarseness were increased in trees subjected to flexures.

Flexure altered wood cell wall chemistry, nanoporosity and saccharification yield

Analysis of the wood by Py-GC/MS indicated elevated G- and H-lignin contents in the flexure set by *c.* 6% and 23%, respectively, resulting in a decrease in the S/G ratio, whereas total carbohydrate and lignin contents were not affected (Fig. 3a). The glycosyl unit composition of the matrix polysaccharides analyzed by acid methanolysis-TMS found that Ara, Xyl and GlcA contents were reduced whereas the contents of Gal, Glc and Man were increased in the flexed trees (Fig. 3b). Moreover, the crystalline cellulose content determined by the Updegraff method showed a 16% increase in flexed compared with stationary trees (Fig. 3c). Intriguingly, when nanoporosity of cell wall material was assayed by BET, a significantly greater (by 24%) specific surface area was observed for flexed trees (Fig. 3d).

To determine whether these changes had any effects on biomass recalcitrance to saccharification, we performed two analytical saccharification experiments on biomass without and with acidic pretreatment (Figs 4a–d, S2). Glc production rate was 21% higher in the flexure set compared with stationary set for the untreated biomass but it was not affected by growth condition for the pretreated biomass. The enzymatic hydrolysis yields from the untreated material indicated significantly increased yields for Glc (+16%) and Gal (+25%; Fig. 4b). Acid hydrolysis liberated more Gal (+40%) and Man (+18%) from flexure than normal wood (Fig. 4c), which was more than expected based on their higher content in flexure wood, whereas the yield of Xyl was not affected by flexure treatment despite the treatment causing a significant decrease in Xyl content. This indicates that matrix polysaccharides from flexure wood are easier to hydrolyze by acid compared with normal wood. The enzymatic hydrolysate after acid pretreatment contained mainly Glc and its yields did not show any significant alterations between the two growth conditions (Fig. S2). The total Glc and Xyl yields (i.e. the sum of pretreatment liquid and enzymatic hydrolysis fractions) were not affected by the growth conditions (Fig. 4d).

Low-intensity stem flexing alters the hormone profiles of tree stems

To gain insight into changes in hormonal profiles of trees exposed to regular low-intensity stem flexures relative to the stationary trees, we performed general hormonomics analysis in cambial region tissues (denoted 'cambium') and developing xylem tissues (denoted 'xylem'), which targeted different forms of cytokinins (CKs), auxins, jasmonates, as well as salicylic acid (SA), abscisic

© 2023 The Authors
New Phytologist © 2023 New Phytologist Foundation

14698137, 0, Downloaded from https://nph.onlinelibrary.wiley.com/doi/10.1111/nph.19307 by Swedish University Of Agricultural Sciences, Wiley Online Library on [15/11/2023]. See the Terms and Conditions (https://onlinelibrary.wiley.com/terms-and-conditions) on Wiley Online Library for rules of use; OA articles are governed by the applicable Creative Commons License

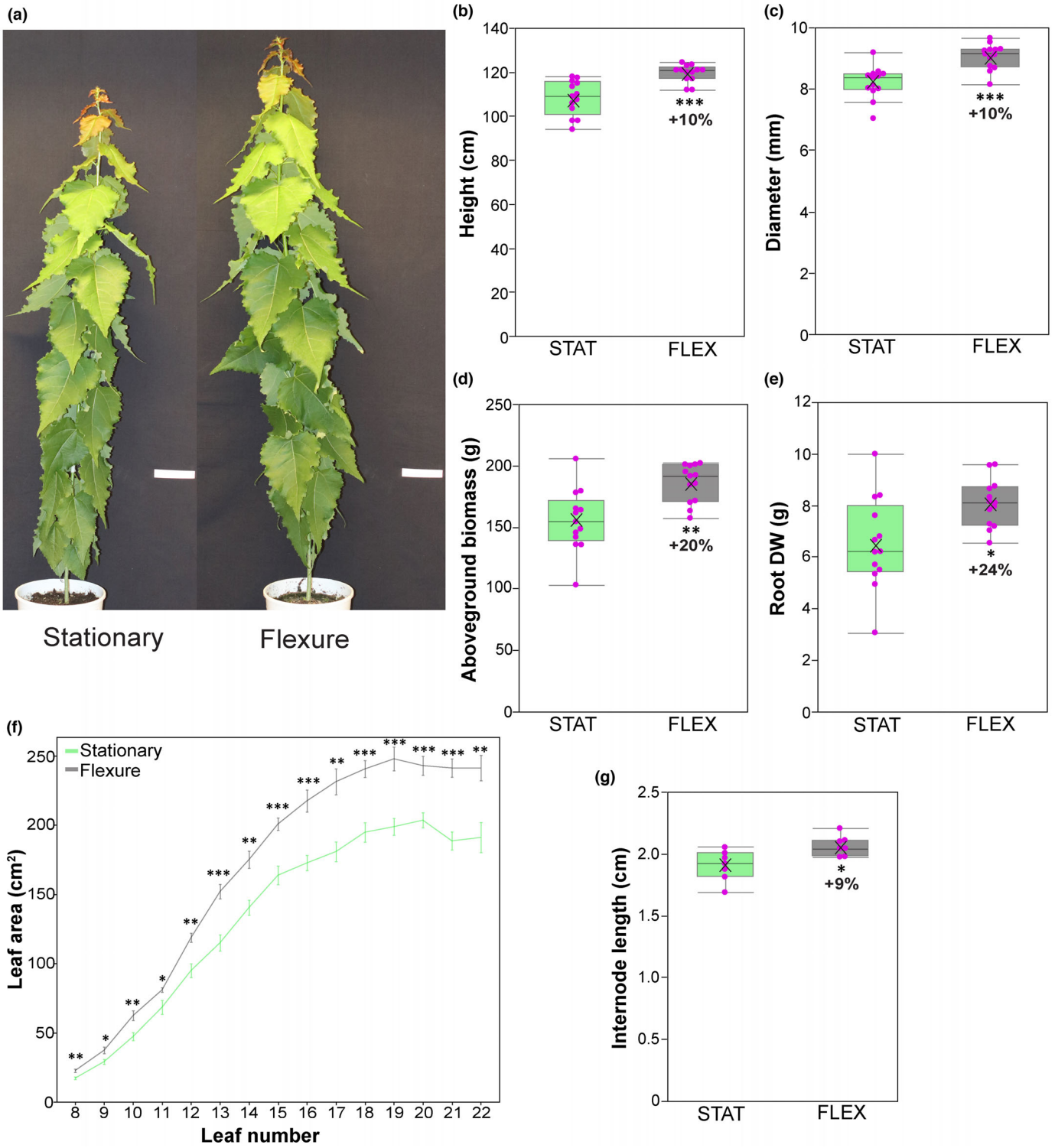

Fig. 1 Effects of hybrid aspen (*Populus tremula* × *tremuloides*) stem flexing on growth. (a) Representative individuals of aspen grown either in the stationary condition (STAT) or subjected to regular low-intensity multidirectional stem flexing (FLEX; as shown in Supporting Information Video S1). Bars, 10 cm. Stem height (b) and diameter (c), aboveground biomass (d), air-dried root biomass (e), leaf area (f) and internode length (g) were measured after five and a half weeks of growth under contrasting conditions. The data are means (±SE), $n = 13$ (b–e) or 7 (f–g). Asterisks denote significance assessed by Student's *t*-test for comparison between flexure and stationary set (*, $P < 0.05$; **, $P < 0.01$; ***, $P < 0.001$). Box plots show interquartile ranges (IQRs) as boxes, medians as horizontal lines, means as crosses, data points as dots, and ranges of all data points as whiskers, except for outliers (points further from the box than 1.5 times IQR).

© 2023 The Authors
New Phytologist © 2023 New Phytologist Foundation

14698137, 0, Downloaded from https://nph.onlinelibrary.wiley.com/doi/10.1111/nph.19307 by Swedish University Of Agricultural Sciences, Wiley Online Library on [15/11/2023]. See the Terms and Conditions (https://onlinelibrary.wiley.com/terms-and-conditions) on Wiley Online Library for rules of use; OA articles are governed by the applicable Creative Commons License

acid (ABA) and the ethylene precursor 1-aminocyclopropane-1-carboxylic acid (ACC) and PAs with their precursors (for list see Table S2). In the cambium, many CK forms were decreased by flexing, whereas in the developing xylem, some forms were increased while others decreased (Fig. 5a,b). Among the auxins, the only significant change upon flexure was a 26% reduction in oxIAA – an IAA catabolite in the xylem. By contrast, distinct changes were detected in hormones mediating abiotic and biotic stresses. Approximately 20% less ABA and SA were detected in the cambium and in the xylem, respectively, and ACC was

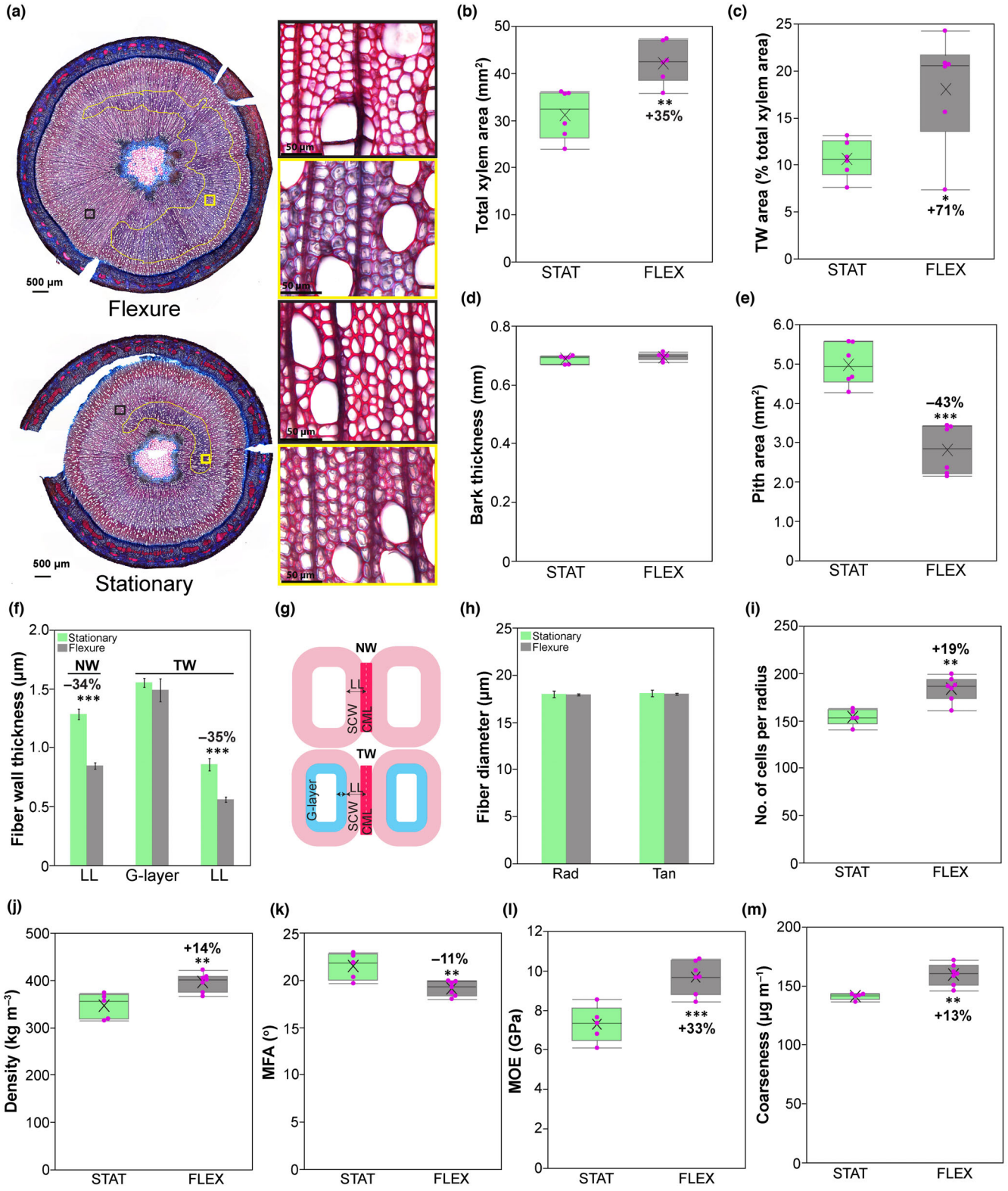

© 2023 The Authors
New Phytologist © 2023 New Phytologist Foundation

14698137, 0, Downloaded from https://nph.onlinelibrary.wiley.com/doi/10.1111/nph.19307 by Swedish University Of Agricultural Sciences, Wiley Online Library on [15/11/2023]. See the Terms and Conditions (https://onlinelibrary.wiley.com/terms-and-conditions) on Wiley Online Library for rules of use; OA articles are governed by the applicable Creative Commons License

14698137, 0, Downloaded from https://nph.onlinelibrary.wiley.com/doi/10.1111/nph.19307 by Swedish University Of Agricultural Sciences, Wiley Online Library on [15/11/2023]. See the Terms and Conditions (https://onlinelibrary.wiley.com/terms-and-conditions) on Wiley Online Library for rules of use; OA articles are governed by the applicable Creative Commons License

Fig. 2 Effects of hybrid aspen (*Populus tremula* × *tremuloides*) stem flexing on wood anatomy and other wood traits determined by SilviScan analyses. (a) Representative transverse stem sections stained by Safranin O and Alcian Blue from flexed and stationary trees. The yellow lines mark the tension wood area and the yellow or black rectangles depict tension or normal wood areas shown in the magnified images. Xylem area (b), tension wood area relative to the total xylem area (c), bark thickness (d) and pith area (e) for six trees from each growth condition. (f) Thickness of different cell wall layers in normal and tension wood fibers (G, gelatinous layer; LL, lignified layer, including secondary cell wall and compound middle lamella layers corresponding to one cell) obtained from measurements of 10 randomly selected fibers in cross-sections from each of six trees per set. (g) Schematic illustration of fiber cells in normal and tension wood indicating the different cell wall layers used for fiber wall thickness measurements. Various wood traits including fiber radial and tangential diameters (h), number of xylem cells per radius (i), wood density (j), MFA (k), MOE (l) and coarseness (m) determined by SilviScan analysis at radial resolution of 25 μm. Data are means (±SE), $n = 5$ (stationary) or 7 (flexure) trees. Asterisks show the significance levels assessed by Student's *t*-test for comparison between flexure and stationary set (*, $P < 0.05$; **, $P < 0.01$; ***, $P < 0.001$). Box plots show interquartile ranges (IQRs) as boxes, medians as horizontal lines, means as crosses, data points as dots, and ranges of all data points as whiskers, except for outliers (points further from the box than 1.5 times IQR). MFA, microfibril angle; MOE, modulus of elasticity; NW, normal wood; TW, tension wood.

reduced by *c*. 38% in both tissues when the trees were exposed to stem flexures. However, the most striking alterations in hormone levels were observed for the jasmonates and PAs. The content of *cis*-12-oxophytodienoic acid (*cis*OPDA), a precursor for JA, was strongly reduced in the cambium and xylem (by 50% and 71%, respectively), whereas that of JA was massively increased (by 266% and 572%, respectively) in flexed trees. Moreover, the content of the biologically active JA-Ile was increased by nearly 50% in the xylem upon mechanical stimuli. These data indicate a metabolic conversion of *cis*OPDA toward JA and the active JA-Ile in the developing xylem in response to the mechanical treatment. In the case of PAs, we found strong decreases in their early precursors, arginine (Arg) in the cambium and glutamic acid (Glu) in the xylem, and an over twofold increase in their downstream precursor – ornithine (Orn) – and in active form – spermidine (Spd), in the xylem, indicating that stem flexing increases PA signaling in the developing xylem.

Complex transcriptional changes in aspen tree stems subjected to flexure

RNA-Seq analysis identified 167 and 219 differentially expressed genes (DEGs) uniquely affected by flexure in the cambium and in the developing xylem, respectively, and 27 genes commonly affected in both tissues (Fig. 6a; Tables S3, S4). In the cambium, the majority of DEGs (75%) were downregulated by the flexing treatment, whereas in the xylem there were similar numbers of up- and downregulated genes. The most strongly affected genes are listed in Table 1.

Gene Ontology enrichment analysis of DEGs in the cambium revealed changes in categories 'generation of precursor metabolites and energy', 'photosynthesis' and closely related categories with the majority of corresponding genes downregulated (Fig. S3; Tables S3, S5). Reduction in expression of photosynthesis-related genes was also reported following a single stem bending in poplar (Pomiès *et al.*, 2017).

In the xylem, GO categories related to cell wall organization and biosynthesis were most highly affected, with the majority of corresponding genes upregulated (Tables 2, S4–S7; Fig. S3). Stem flexure stimulated expression of primary wall CesAs *PtCESA6-A* and *PtCESA6-F* (Fig. S4; Suzuki *et al.*, 2006; Desprez *et al.*, 2007; Kumar *et al.*, 2009; Hu *et al.*, 2018; Zhang *et al.*, 2018) and genes involved in microtubule organization, such as *PtMAP20* (Rajangam *et al.*, 2008). Noteworthy, primary wall CesAs were reported in developing wood cells depositing secondary cell walls (Song *et al.*, 2010). Elevated transcript levels were observed for genes encoding pectin acetylesterases homologous to *AtPAE8* and *AtPAE12* (de Souza *et al.*, 2014), and pectin methylesterases (PMEs) homologous to *AtPME41* and *AtPMEI-PME20*, whereas a homolog of *AtPMEI-PME18* along with two polygalacturonase-encoding genes, *PtPG28* and *PtPG41*, were downregulated in the xylem. Interestingly, *AtPMEI-PME18* is the main PME downregulated under microgravity (Xu *et al.*, 2022). Several xyloglucan transglycosidases/hydrolases (XTH) were upregulated by flexure, in agreement with the proposed role of this family in touch responses in Arabidopsis (Xu *et al.*, 1995; Lee *et al.*, 2005). One of them, *PtXTH37* (*AtXTH23*; Fig. S5), was among the most highly upregulated genes in the cambium (Table 1) and 2 h after a single stem bending (Pomiès *et al.*, 2017). Several genes encoding xylan *O*-acetyltransferases known to be involved in regiospecific *O*-acetylation of xylan (Zhong *et al.*, 2017, 2018) were upregulated in the xylem by stem flexing, including *PtXOAT1* (*AtESK1/TBL29*), *PtXOAT7* (*AtTBL3*) and *PtXOAT8* (*AtTBL31*). In addition, a putative xylan acetylesterase of the CE6 family showed upregulation upon stem flexure in the xylem, as was also seen during tension wood formation (Andersson-Gunnerås *et al.*, 2006). However, among other xylan biosynthetic genes, only *PtGATL2-A* (*AtGATL1/PARVUS*) involved in reducing sequence biosynthesis (Lee *et al.*, 2007, 2009) and *PtGXM3* (*AtGXMT1*) involved in glucuronosyl methylation (Urbanowicz *et al.*, 2012; Yuan *et al.*, 2014) were slightly upregulated. These changes suggest alteration in xylan acetylation in both flexure and tension wood compared with normal wood. Four out of 17 genes of clade *At*FLA11/FLA12 (Zang *et al.*, 2015) were upregulated by flexure in the xylem, including *PtFLA6*, which has been implicated in tension wood formation (Wang *et al.*, 2017). This clade is involved in G-layer biosynthesis (Lafarguette *et al.*, 2004; Andersson-Gunnerås *et al.*, 2006), and it was also reported to be upregulated after single stem bending (Pomiès *et al.*, 2017). Genes encoding laccases *PtLAC21* and *PtLAC49* (*AtLAC4*), *PtLAC12* (*AtLAC17*; Berthet *et al.*, 2011; Lu *et al.*, 2013; Kumar *et al.*, 2019) and a class III peroxidase *PtPRX67* (Ren *et al.*, 2014) likely involved in lignin polymerization, and genes involved in monolignol metabolism and transport were also upregulated in either xylem or cambium of flexed trees (Franke *et al.*, 2002; Kaneda *et al.*, 2011; Lin *et al.*, 2016; Table 2). By contrast, the genes encoding three other class III peroxidases, including a homolog of *AtPRX72* responsible for lignification in Arabidopsis stems (Fernández-Pérez *et al.*, 2015; Hoffmann *et al.*, 2020), were

© 2023 The Authors
New Phytologist © 2023 New Phytologist Foundation

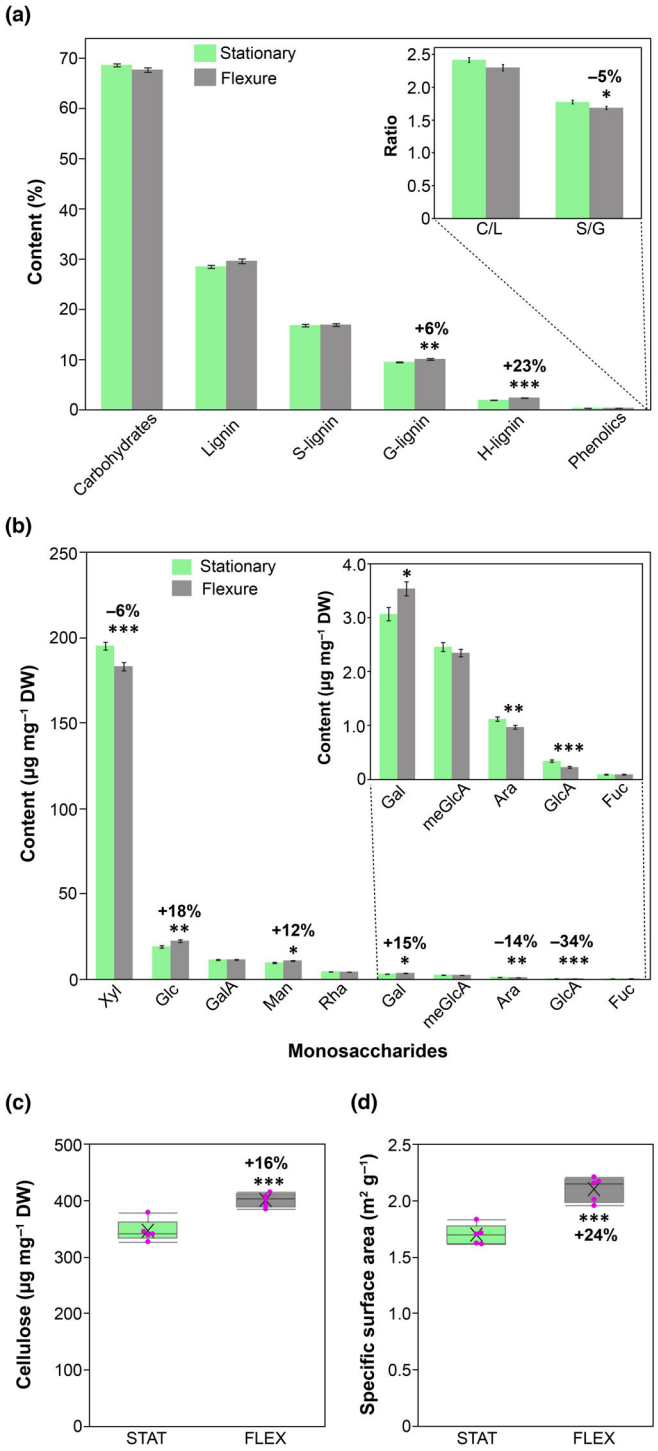

Fig. 3 Effects of hybrid aspen (*Populus tremula* × *tremuloides*) stem flexing on wood chemistry. (a) Py-GC/MS results reveal changes in wood chemical composition according to the different identified compounds present in the material. Carbohydrates to lignin as well as S-lignin to G-lignin ratios are presented in the top right corner of the chart. (b) Monosaccharide (anhydrous form) composition by TMS analysis of aspen wood material. The bars representing the sugars with relatively low amounts are shown in the inset. Data in (a) and (b) are means (±SE), $n = 7$ biological replicates. (c) Crystalline cellulose content measured by the Updegraff method. (d) Specific surface area (SSA) determined by BET nanoporosity assay. Data in (c) and (d) are means (±SE) of $n = 5$ technical replicates from pooled wood material from seven trees. Asterisks show the significance of the differences between growth conditions assessed by Student's *t*-test (*, $P < 0.05$; **, $P < 0.01$; ***, $P < 0.001$). Box plots show interquartile ranges (IQRs) as boxes, medians as horizontal lines, means as crosses, data points as dots, and ranges of all data points as whiskers, except for outliers (points further from the box than 1.5 times IQR). Ara, arabinose; Fuc, fucose; Gal, galactose; GalA, galacturonic acid; Glc, glucose; GlcA, glucuronic acid; Man, mannose; meGlcA, methylglucuronic acid; Rha, rhamnose; Xyl, xylose.

strongly downregulated. These peroxidases, however, were relatively lowly expressed in aspen wood-forming tissues. This indicates that flexure activates lignification using specific sets of enzymes. In general, the changes in gene expression point to increased cellulose biosynthesis, modified pectin esterification, increased xylan acetylation and lignification.

Both cambium and xylem tissues showed significantly enriched GO terms related to transcriptional and hormonal regulation, but with different specificities (Tables 1, 3, S3–S7; Fig. S3). In the cambium, there was significant enrichment of GO terms including thermospermine synthase activity, and general processes like protein or DNA binding and response to abiotic stimulus, whereas in the xylem, there was enrichment for processes related to auxin, GAs, jasmonates and the osmosensor activity. Some of the most highly affected genes were within these categories. In the cambium, a homolog of *AtACL5* encoding a thermospermine synthase in the PA biosynthetic pathway (Kakehi *et al.*, 2008; Muñiz *et al.*, 2008) exhibited higher expression upon stem flexures whereas an arginine decarboxylase (*AtADC1*) was *de novo* induced in the xylem along with downregulation of a PA oxidase (*AtPAO1*). These changes suggest increased PA levels in flexed stems. Furthermore, reduced expression in the xylem was observed for the homolog of the type-B response regulator *AtRR12* mediating CK responses (Yokoyama *et al.*, 2007), suggesting suppressed CK signaling upon stem flexures, which is in agreement with the general decrease in CKs observed in the cambium (Fig. 5a). Reductions in transcripts encoding several ABA biosynthetic enzymes were observed in both tissues (Table 3), including a homolog of *AtNCED3* (Iuchi *et al.*, 2001), and an increase in transcripts related to ABA catabolism homologous to *AtCYP707A4* (Kushiro *et al.*, 2004) in the xylem, indicating reduced ABA levels, which was in agreement with the hormonomics results (Fig. 5b). Moreover, several ABA-related TFs and signaling components such as homolog of *AtRD26* (Jiang *et al.*, 2019) were downregulated in the cambium (Tables 1, 3, S6). By contrast, genes related to BR biosynthesis and regulation were upregulated including a homolog of *AtDWF4/CYP90B1* (Fujita *et al.*, 2006), *AtEXO* and *AtEXL5* (Schröder *et al.*, 2009). In the xylem, a homolog of *AtBARK1/TMK4* encoding a kinase negatively regulating auxin biosynthesis (Wang *et al.*, 2020a) was one of the most upregulated genes by stem flexing and homologs of different auxin transporters *AtPIN1*, *AtLAX3* and *AtAUX1* were affected whereas in the cambium, increased transcript levels of phosphatidylinositol transfer patellins involved in *At*PIN1 relocation (Tejos *et al.*, 2018) indicated changes in auxin transport upon stem flexures. Ethylene

© 2023 The Authors
New Phytologist © 2023 New Phytologist Foundation

14698137, 0, Downloaded from https://nph.onlinelibrary.wiley.com/doi/10.1111/nph.19307 by Swedish University Of Agricultural Sciences, Wiley Online Library on [15/11/2023]. See the Terms and Conditions (https://onlinelibrary.wiley.com/terms-and-conditions) on Wiley Online Library for rules of use; OA articles are governed by the applicable Creative Commons License

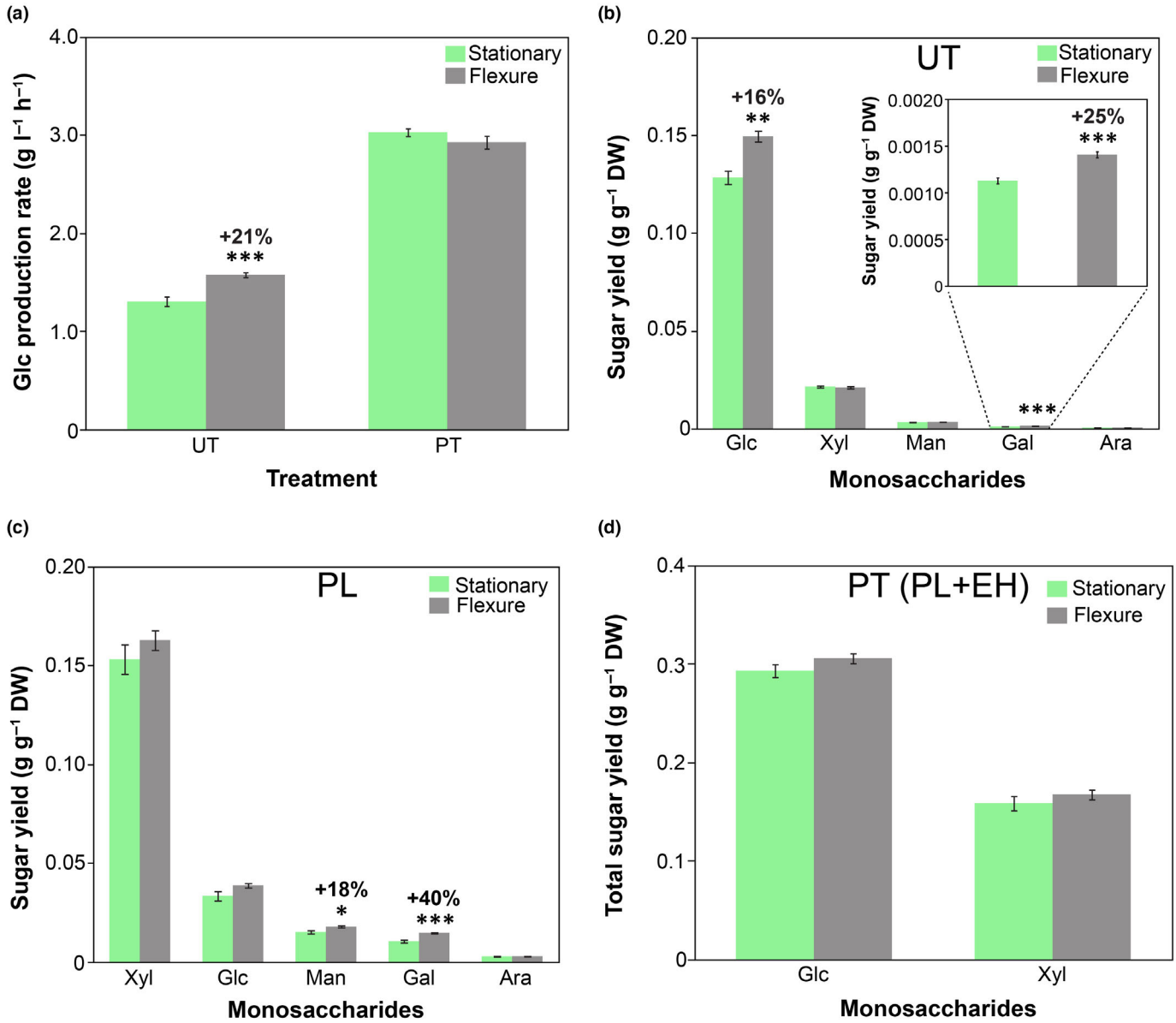

Fig. 4 Effects of hybrid aspen (*Populus tremula* × *tremuloides*) stem flexing on wood recalcitrance. Glc production rates for saccharification without pretreatment (a, left) and with acidic pretreatment (a, right). (b) Sugar yield of biomass in enzymatic hydrolysate following saccharification assay of untreated wood. The significant change in Gal yield is shown in the inset for better interpretation. (c) Sugar yield of biomass in pretreatment liquid fraction following thermochemical hydrolysis of wood during acidic pretreatment. (d) Total sugar yield of biomass for Glc and Xyl after acidic pretreatment. Data are means (±SE) of $n = 5$ technical replicates from pooled wood material from seven trees. Asterisks show the significance of the differences between growth conditions assessed by Student's *t*-test (*, $P < 0.05$; **, $P < 0.01$; ***, $P < 0.001$). Ara, arabinose; EH, enzymatic hydrolysate; Gal, galactose; Glc, glucose; Man, mannose; PL, pretreatment liquid; PT, pretreated; UT, untreated; Xyl, xylose.

biosynthesis and signaling appered to be stimulated by the mechanical stimuli since transcripts encoding ACC oxidase – the key ethylene biosynthetic gene – homologous to *AtACO4/EFE* were among the most upregulated in the xylem whereas some negative regulators of ethylene signaling, such as homologs of *AtEBF2* and *AtERF4* (Yang *et al.*, 2005; Li *et al.*, 2015), were downregulated in the cambium. Altered GA signaling in the xylem of flexed stems was evidenced by strong upregulation of aspen homologs of gibberellin 2-oxidase *AtGA2OX6* involved in GA catabolism (Lange & Lange, 2015) and GA-stimulated protein *AtGASA14*. Despite the remarkable increase in JA and JA-Ile content upon stem flexures (Fig. 5), we did not find a significant upregulation of transcripts in the jasmonate biosynthesis pathway. Homologs of *AtJAR1* involved in the formation of biologically active JA-Ile (Staswick & Tiryaki, 2004) and *AtJAZ3* (*Potra2n10c21496*) mediating downstream jasmonate responses (Liu *et al.*, 2021) exhibited decreased expression in the xylem (Table 3).

Mechanical stimuli also caused alterations in transcript levels of genes involved in Ca^{2+}, G-protein and receptor-like kinase (RLK) signaling (Table 3). For instance, the *CML* gene homologous to *AtCML5/MSS3*, which is induced by touch in

© 2023 The Authors
New Phytologist © 2023 New Phytologist Foundation

14698137, 0, Downloaded from https://nph.onlinelibrary.wiley.com/doi/10.1111/nph.19307 by Swedish University Of Agricultural Sciences, Wiley Online Library on [15/11/2023]. See the Terms and Conditions (https://onlinelibrary.wiley.com/terms-and-conditions) on Wiley Online Library for rules of use; OA articles are governed by the applicable Creative Commons License

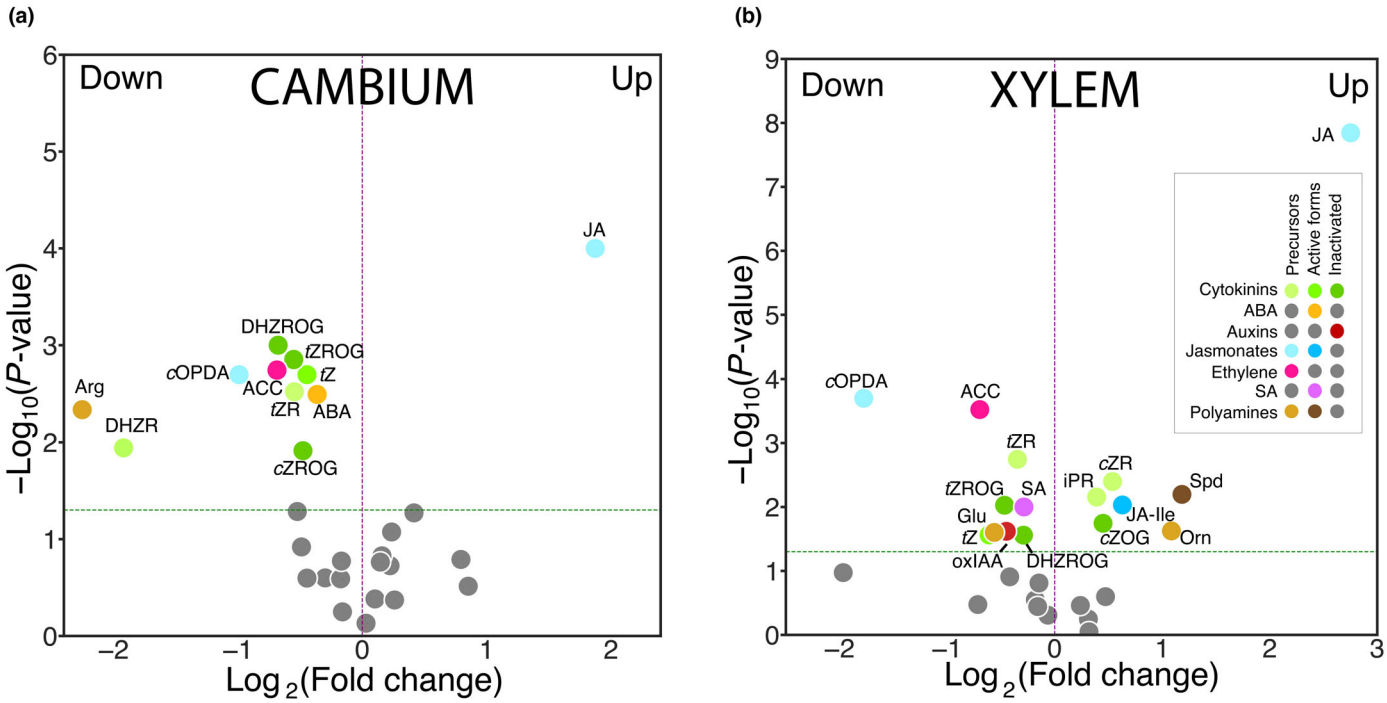

Fig. 5 Hormonal alterations in hybrid aspen (*Populus tremula* × *tremuloides*) upon regular stem flexures. Volcano plots depict the changes in the mean ($n = 5$ for polyamines or 4 for remaining compounds) hormone concentrations (pmol g^{-1} FW) of the different targeted compounds analyzed in the cambial region tissues (cambium) (a) and developing xylem tissues (xylem) (b) in the flexure-treated trees as compared with the stationary trees. Gray dots without labels represent the detected compounds that did not meet the significance criteria ($P < 0.05$, Student's *t*-test). Colored dots with names show the hormones that were either significantly increased ('Up') or reduced ('Down') in the flexure set compared with the stationary trees. ABA, abscisic acid (active); ACC, 1-aminocyclopropane-1-carboxylic acid (precursor); Arg, arginine (precursor); *c*OPDA, *cis*-12-oxophytodienoic acid (precursor); *c*ZOG, *cis*-zeatin-*O*-glucoside (inactivated); *c*ZR, *cis*-zeatin riboside (precursor); *c*ZROG, *cis*-zeatin riboside-*O*-glucoside (inactivated); DHZR, dihydrozeatin riboside (precursor); DHZROG, dihydrozeatin riboside-*O*-glucoside (inactivated); Glu, glutamic acid (precursor); iPR, N^6-isopentenyladenine riboside (precursor); JA, jasmonate (precursor); JA-Ile, jasmonate-isoleucine conjugate (active); Orn, ornithine (precursor); oxIAA, 2-oxoindole-3-acetic acid (inactivated); SA, salicylic acid (active); Spd, spermidine (active); *t*Z, *trans*-zeatin (active); *t*ZR, *trans*-zeatin riboside (precursor); *t*ZROG, *trans*-zeatin riboside-*O*-glucoside (inactivated).

Arabidopsis (Lee *et al.*, 2005), had greater expression in the cambium of flexed vs stationary stems. An aspen homolog of a leucine-rich repeat RLK *AtXIP1/CEPR1*, a receptor of C-terminally encoded peptides involved in vascular development (Bryan *et al.*, 2012), exhibited almost a six-fold downregulation in the xylem, whereas a homolog of *AtRLK902* encoding a RLK mediating BR responses (Zhao *et al.*, 2019) was upregulated. In the cambium of flexed stems, several genes related to cell division and growth were upregulated such as homologs of *AtCYCP3*;2 – a cyclin regulating cell division cycle (Torres Acosta *et al.*, 2004), and *AtWLIM1* (Table S3) from the LIM family involved in cytoskeleton organization and known to be involved in tension wood formation (Arnaud *et al.*, 2007).

Among the TFs with altered expression in the xylem (Table S6), the simultaneous upregulation of homologs of *AtMYB52*, *AtKNAT3*, as well as the tandem CCCH zinc finger transcriptional activators *AtC3H14* and *AtC3H15/CDM1* that regulate secondary cell wall formation in the xylem (Zhong *et al.*, 2008; Zhong & Ye, 2012; Cassan-Wang *et al.*, 2013; Kim *et al.*, 2013; Chai *et al.*, 2015; Wang *et al.*, 2020b), further indicate sophisticated control over secondary cell wall deposition during mechanical stimuli in aspen. Three genes encoding C2H2-type zinc finger proteins were also affected by flexure in the xylem, including a homolog of *AtZAT5* related to the previously identified stem bending marker *ZFP2* (Fig. S6; Leblanc-Fournier *et al.*, 2008; Martin *et al.*, 2009).

Differentially expressed genes in stems subjected to flexure form co-expression networks in stems of field-grown trees

To reveal the co-expression networks among the genes differentially expressed in the wood-forming tissues of flexed stems, we analyzed their networks within the developing wood of field-grown aspen naturally exposed to stem flexures using the AspWood database (Sundell *et al.*, 2017). Five and three clusters of co-expressed genes were found for the cambium and xylem DEGs, respectively, and their expression patterns were shown as heatmaps (Fig. 6a–c; Table S8). Xylem cluster 1 and cambium cluster 5 included genes that were upregulated by flexing while the remaining clusters included downregulated genes, identifying candidates for positive or negative regulators of flexure wood formation, respectively. Xylem cluster 1 included genes expressed at the onset of secondary wall formation. It contained several TFs, notably zinc finger TFs such as homologs of the putative mechanoperception regulator *AtZAT5* and secondary cell wall biosynthesis regulators *AtC3H14* and *AtC3H15*. It also contained

© 2023 The Authors
New Phytologist © 2023 New Phytologist Foundation

14698137, 0, Downloaded from https://nph.onlinelibrary.wiley.com/doi/10.1111/nph.19307 by Swedish University Of Agricultural Sciences, Wiley Online Library on [15/11/2023]. See the Terms and Conditions (https://onlinelibrary.wiley.com/terms-and-conditions) on Wiley Online Library for rules of use; OA articles are governed by the applicable Creative Commons License

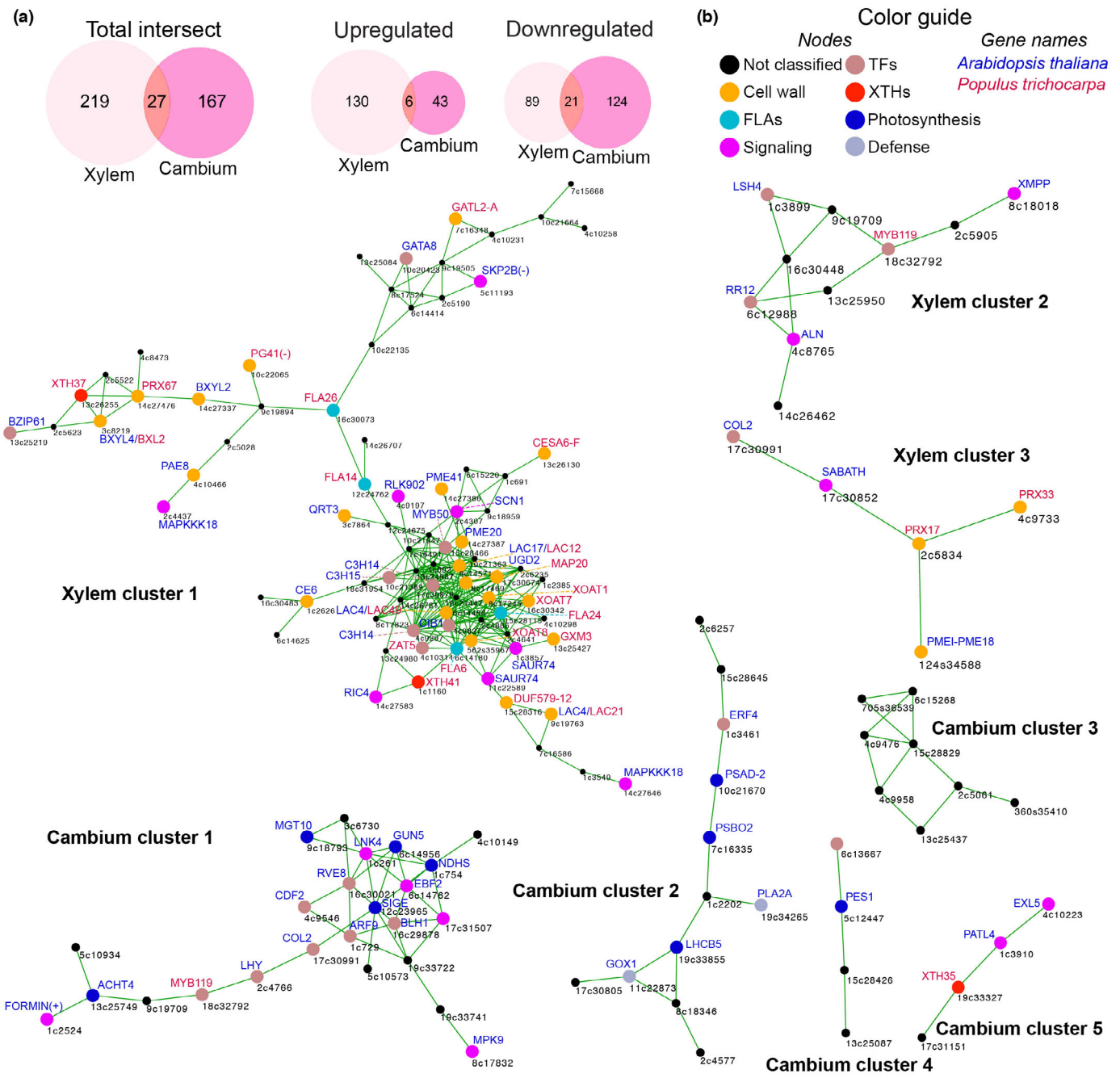

Fig. 6 Transcriptional changes in hybrid aspen (*Populus tremula* × *tremuloides*) stems in response to flexure. (a) Venn diagrams represent the total number of differentially expressed genes (DEGs, FC ≥ 1.5) in the xylem and cambium from aspen stems subjected to low-intensity stem flexures relative to the stationary stems. (b) Co-expression clusters, based on the AspWood database (Sundell *et al*., 2017) of DEGs in xylem and cambium tissues. The gene names are shown for *Arabidopsis thaliana* (blue) and/or *Populus trichocarpa* (red), also the color guide explains the differently colored nodes indicating various categories the DEGs were assigned to. Codes beside the nodes correspond to Potra2n gene ID. (c) Heatmaps indicating the AspWood expression patterns of the genes from the clusters shown in (b). Ca, cambium and radial expansion zone; PCD, lignification and programmed cell death; Ph, phloem; PW-SW, primary to secondary wall transition zone; SW, secondary wall deposition zone; numbers 01–25 above the heatmaps correspond to the sample number for tree 1 in AspWood; genes are identified by their Potra2n IDs on the right.

signaling-related genes such as homologs of *AtSKP2B* and *AtRLK902*, four *AtFLA11/FLA12* homologs, *PtXTH37* and *41*, as well as xylan and pectin acetylation-related genes. Remarkably, the expression pattern of *SKP2B* in developing wood was opposite to other genes of this cluster and this gene was negatively regulated by flexing. Its product functions as a part of E3 ubiquitin ligase SCF complex negatively regulating the level of E2FC TF, which is a key regulator of cambial cell division and secondary cell wall formation in Arabidopsis (Manzano *et al*., 2012; Taylor-Teeples *et al*., 2015). Xylem cluster 2 included genes

© 2023 The Authors
New Phytologist © 2023 New Phytologist Foundation

14698137, 0, Downloaded from https://nph.onlinelibrary.wiley.com/doi/10.1111/nph.19307 by Swedish University Of Agricultural Sciences, Wiley Online Library on [15/11/2023]. See the Terms and Conditions (https://onlinelibrary.wiley.com/terms-and-conditions) on Wiley Online Library for rules of use; OA articles are governed by the applicable Creative Commons License

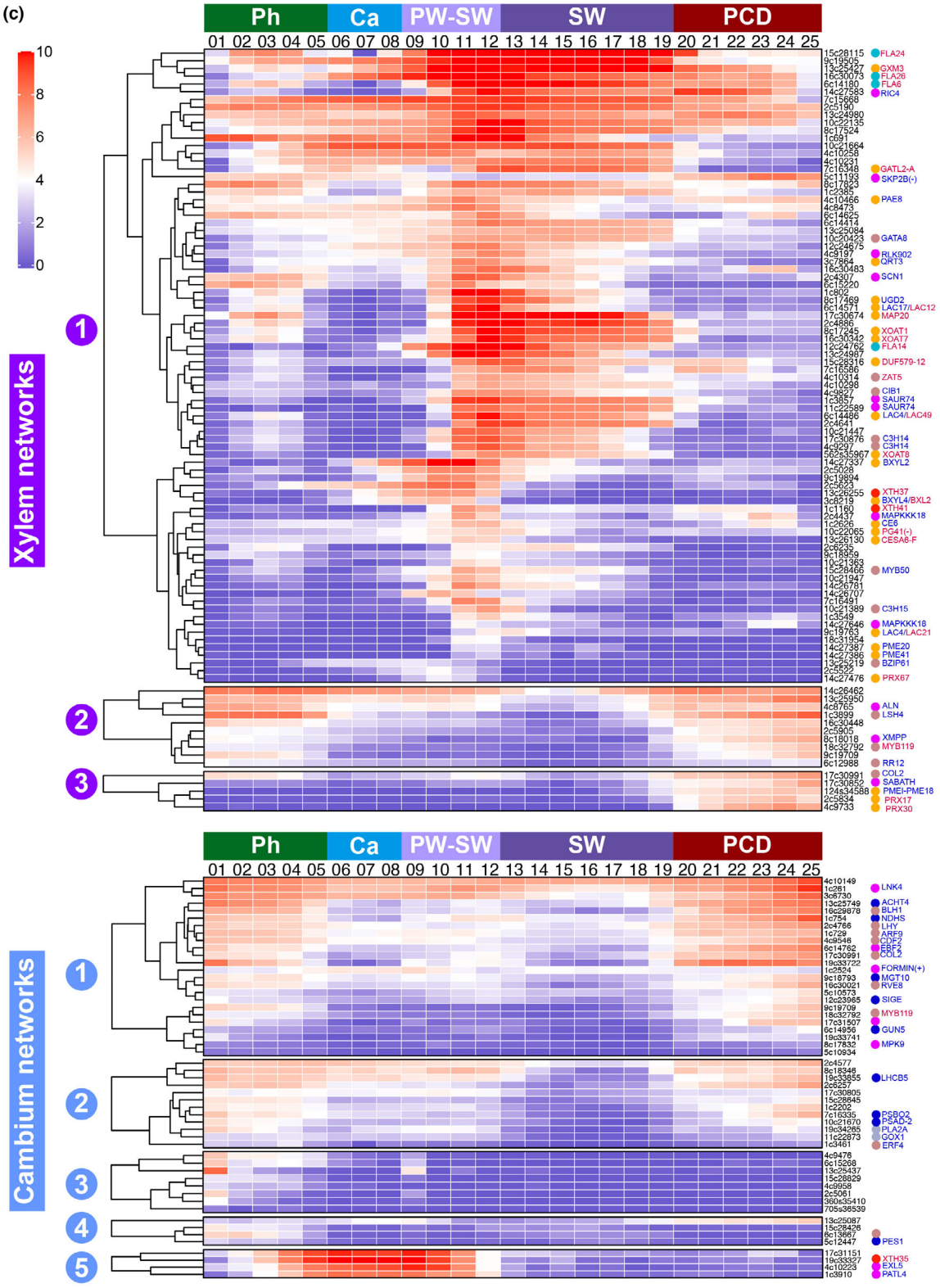

Fig. 6 (Continued)

expressed in the phloem and in the xylem programmed cell death (PCD) zone, comprising the CK regulator *AtRR12* and homologs of genes encoding enzymes related to purine catabolism, *AtXMPP* (Heinemann *et al.*, 2021) and *AtALN* (Takagi *et al.*, 2016), regulating the steady-state of allantoin, a stress-related metabolite that activates JA signaling. Xylem cluster 3 included genes expressed

© 2023 The Authors
New Phytologist © 2023 New Phytologist Foundation

14698137, 0, Downloaded from https://nph.onlinelibrary.wiley.com/doi/10.1111/nph.19307 by Swedish University Of Agricultural Sciences, Wiley Online Library on [15/11/2023]. See the Terms and Conditions (https://onlinelibrary.wiley.com/terms-and-conditions) on Wiley Online Library for rules of use; OA articles are governed by the applicable Creative Commons License

14698137, 0, Downloaded from https://nph.onlinelibrary.wiley.com/doi/10.1111/nph.19307 by Swedish University Of Agricultural Sciences, Wiley Online Library on [15/11/2023]. See the Terms and Conditions (https://onlinelibrary.wiley.com/terms-and-conditions) on Wiley Online Library for rules of use; OA articles are governed by the applicable Creative Commons License

Table 1 List of the five most up- and downregulated differentially expressed genes (DEGs; $P \leq 0.05$ and fold change expression ≥ 1.5) in the cambium and xylem tissues of mechanically stimulated hybrid aspen (*Populus tremula* × *tremuloides*) stems compared with the stationary set.

Potra v.2.2 gene ID*	Log_2 FC	Potri v.3.1 gene ID**	*Populus* name***	CAZy***	AGI gene ID****	AGI gene name	Description (TAIR, www.arabidopsis.org/)
Cambium							
Potra2n14c27099	1.5	Potri.014G096000		GT1	AT4G01070	UGT72B1	UDP-glucosyltransferase
Potra2n12c24367	1.4	Potri.002G022500			AT5G14920	GASA14	Gibberellin-stimulated protein
Potra2n5c11397	1.3	Potri.002G098800			AT4G08950	EXO	Exordium
Potra2n1c2524	1.2	Potri.001G288900			AT1G10020		Formin-like protein (DUF1005)
Potra2n13c26255	1.1	Potri.013G005700	XTH37	GH16	AT4G25810	XTH23/XTR6	XTH
Potra2n11c22767	−3.0	Potri.011G123300			AT4G27410	RD26/ ANAC72	NAC transcription factor
Potra2n4c9958	−3.0	Potri.004G172300			AT2G17880	DJC24	Chaperone DNAJ-domain protein
Potra2n13c25439	−3.2	Potri.013G100800			AT4G24350		Phosphorylase family protein
Potra2n13c25212	−3.6	Potri.013G125300			AT3G25180	CYP82G1	Cytochrome P450 monooxygenase
Potra2n13c25437	−4.7	Potri.013G100800			AT4G24340		Phosphorylase family protein
Xylem							
Potra2n1022s36932	9.2	Potri.004G163300			AT2G16500	ADC1	Arginine decarboxylase
Potra2n13c25987	1.8	Potri.013G035900			AT3G23750	BARK1/ TMK4	Receptor-like kinase
Potra2n747s36676	1.6	Potri.002G224100			AT1G05010	ACO4/EFE	ACC oxidase
Potra2n12c24367	1.5	Potri.002G022500			AT5G14920	GASA14	Gibberellin-stimulated protein
Potra2n14c27286	1.4	Potri.014G117300			AT1G02400	GA2OX6	Gibberellin 2-oxidase
Potra2n2c5061	−3.9	Potri.002G150400			AT2G45550	CYP76C4	Geraniol 9- or 8-hydroxylase
Potra2n2c6318	−4.3	Potri.002G015100			AT3G03190	GSTF11	Glutathione S-transferase
Potra2n2c4331	−4.4	Potri.002G233200			AT5G16740		Amino acid transporter
Potra2n7c16468	−4.5	Potri.005G118700			AT5G66390	PRX72	Peroxidase
Potra2n1398s37044	−5.4	Potri.011G016400			AT3G18670		Ankyrin repeat family protein

**Populus tremula* v.2.2 gene ID.
**Best DIAMOND Potri gene ID based on Potra v.2.2 gene ID.
***CAZy, carbohydrate-active enzymes and gene name (Kumar *et al.*, 2019).
****Best DIAMOND AGI gene ID based on Potra v.2.2 gene ID; FC, fold change (flexure/stationary expression).

in the PCD zone where stress-related peroxidases and a homolog of *AtPMEI-PME18* were suppressed by flexing. Cambium clusters 1 and 2 exhibited upregulation in the phloem and PCD zone, similar to xylem cluster 2. Functionally however, these clusters differed by having large numbers of photosynthesis-related genes. Cambium cluster 1 also included genes encoding TFs and signaling proteins related to ABA (similar to *AtBLH1* and *AtMPK9*), auxin (similar to *AtARF9*), CK (similar to *AtCOL2*) and ethylene (similar to *AtEBF2*) responses. Cambium cluster 5 was distinct by including genes highly and specifically expressed in the cambium and radial expansion zone that were upregulated by flexing. They included a homolog of *AtPATL4* involved in PIN1 relocation and genes encoding cell wall-localized proteins involved in cell proliferation and growth, such as a homolog of *AtEXL5* involved in BR responses and *PtXTH35* (*AtXTH9*), the most abundant XTH in wood-forming tissues mediating xylem cell size (Kushwah *et al.*, 2020).

Discussion

Plants perceive both internal and external mechanical cues to adjust their growth and development (Alonso-Serra *et al.*, 2020; Moulia *et al.*, 2021). Low-intensity stem flexure stress induced by wind is an everyday mechanical perturbance encountered by young trees. In the present study, we investigated the effects of multiple low-intensity stem flexures mimicking wind sway in aspen to advance our understanding of tree growth, and to reveal possible signaling pathways involved in these responses.

Low-intensity stem flexing increases growth

We found that gentle stem flexure led to an overall increase in growth (Fig. 1). Root biomass showed the highest increase, indicating augmented biomass allocation to the root, although there was also a prominent increase in leaf size, which largely contributed to the higher aboveground biomass of the flexed trees. Increased stem radial expansion and root growth but reduced stem elongation and leaf growth were reported in mechanically perturbed plants (Telewski & Jaffe, 1986a,b; Telewski & Pruyn, 1998; Coutland *et al.*, 2000, 2008, 2009; Kern *et al.*, 2005; Wu *et al.*, 2016), but this phenotype was not always observed in all studied genotypes (Jaffe, 1973; Telewski & Jaffe, 1986b; Wu *et al.*, 2016; Roignant *et al.*, 2018) or in all types of experiments (Paul-Victor & Rowe, 2011). Stem elongation was shown to be inhibited shortly after mechanical stimulation, followed by growth recovery and/or growth stimulation (Jaffe *et al.*, 1980; Coutand *et al.*, 2000, 2009); thus, the observed growth effect can vary depending on the time the observations are made. Moreover, the extent of plant responses to stem bending has been shown to be correlated with the number of flexures applied, the magnitude of stem longitudinal strain or the bending angle (Jaffe *et al.*, 1980; Telewski & Pruyn, 1998; Coutand *et al.*, 2009). The swaying angle in our experiment was

© 2023 The Authors
New Phytologist © 2023 New Phytologist Foundation

Table 2 Differentially expressed genes (DEGs; $P \leq 0.05$ and fold change expression ≥ 1.5) related to cell wall biosynthesis and modification in the cambium and xylem tissues of mechanically stimulated hybrid aspen (*Populus tremula* × *tremuloides*) stems and their transcriptional behavior (up- or downregulation) relative to the stationary set.

Potra v.2.2 gene ID*	Log_2 FC	Potri v.3.1 gene ID**	*Populus* name***	CAZy***	AGI gene ID****	AGI gene name	Description (TAIR, www.arabidopsis.org/)
Cambium							
Potra2n13c26255	1.1	Potri.013G005700	XTH37	GH16	AT4G25810	XTH23/XTR6	XTH
Potra2n19c33327	0.6	Potri.019G125000	XTH35	GH16	AT4G03210	XTH9	XTH
Potra2n9c18880	1.0	Potri.007G083400	EXPLA2	EXPN	AT4G38400	EXLA1, EXLA2	Expansin-like
Potra2n14c27766	0.8	Potri.014G168100			AT4G12730	FLA2	Fasciclin-like arabinogalactan protein
Potra2n10c22065	−1.1	Potri.010G042100	PG41	GH28	AT1G10640		Polygalacturonase
Potra2n10c22100	0.7	Potri.010G038300	GATL8-B	GT8	AT1G70090	GATL9	Galacturonosyltransferase-like protein
Potra2n16c29485	−1.3	Potra2n16c29485			AT2G40890	REF8	Coumarate 3-hydrolase
Potra2n14c27099	1.5	Potri.014G096000		GT1	AT4G01070	UGT72B1	UDP-glucosyltransferase
Xylem							
Potra2n13c26130	0.8	Potri.013G019800	CesA6-F	GT2	AT5G64740	CESA6/IXR2	Primary wall cellulose synthase
Potra2n5c12058	0.7	Potri.005G087500	CesA6-A	GT2	AT4G39350	CESA2	Primary wall cellulose synthase
Potra2n1c1160	1.0	Potri.001G136100	XTH41	GH16	AT1G32170	XTH30/XTR4	XTH
Potra2n13c26255	0.7	Potri.013G005700	XTH37	GH16	AT4G25810	XTH23/XTR6	XTH
Potra2n5c12814	0.6	Potri.005G001500		CE13	AT3G05910	PAE12	Pectin acetylesterase
Potra2n4c10466	0.6	Potri.004G234100		CE13	AT4G19420	PAE8	Pectin acetylesterase
Potra2n14c27387	1.3	Potri.014G127000		CE8	AT2G47550	PMEI-PME20	Pectin methylesterase inhibitor-PME
Potra2n14c27386	1.0	Potri.014G127000		CE8	AT4G02330	PME41	PME
Potra2n10c22100	0.8	Potri.010G038300	GATL8-B	GT8	AT1G70090	GATL9	Galacturonosyltransferase-like protein
Potra2n8c17469	0.6	Potri.008G094300			AT3G29360	UGD2	UDP-glucose dehydrogenase
Potra2n124s34588	−1.9	Potri.011G025400		CE8	AT1G11580	PMEI-PME18	Pectin methylesterase inhibitor-PME
Potra2n8c17528	−1.5	Potri.008G100500	PG28	GH28	AT1G48100	PGX3	Polygalacturonase
Potra2n3c7864	0.6	Potri.003G074600			AT4G20050	QRT3/PGF11	Polygalacturonase
Potra2n10c22065	−1.0	Potri.010G042100	PG41	GH28	AT1G10640		Polygalacturonase
Potra2n3c8219	0.7	Potri.003G022900	BXL2	GH3	AT5G64570	XYL4	β-D-xylosidase
Potra2n14c27337	0.6	Potri.014G122200		GH3	AT1G02640	BXL2	β-D-xylosidase
Potra2n16c30342	0.6	Potri.016G119100	XOAT7/TBL59		AT5G01360	TBL3	Xylan *O*-acetyltransferase
Potra2n562s35967	0.8	Potri.001G376700	XOAT8/TBL60		AT1G73140	TBL31	Xylan *O*-acetyltransferase
Potra2n5c12326	0.7	Potri.005G060800	TBL27		AT1G48880	TBL7	Likely xylan *O*-acetyltransferase
Potra2n8c17245	0.6	Potri.008G069900	XOAT1/TBL51		AT3G55990	ESK1/TBL29	Xylan *O*-acetyltransferase
Potra2n1c2626	0.6	Potri.009G096400		CE6	AT4G34215		SGNH-hydrolase family protein
Potra2n7c16348	0.7	Potri.007G031700	GATL2-A	GT8	AT1G19300	PARVUS/ GATL1	Galacturonosyltransferase-like
Potra2n13c25427	0.7	Potri.013G102200	GXM3		AT1G33800	GXMT1	Glucuronoxylan 4-*O*-methyltransferase
Potra2n15c28316	0.6	Potri.015G096900			AT4G24910		Glucuronoxylan 4-*O*-methyltransferase-like
Potra2n16c30073	0.7	Potri.016G088700	FLA26		AT5G03170	FLA11	Fasciclin-like arabinogalactan protein
Potra2n6c14180	0.6	Potri.006G129200	FLA6		AT5G03170	FLA11	Fasciclin-like arabinogalactan protein
Potra2n12c24762	0.8	Potri.012G127900	FLA14		AT5G60490	FLA12	Fasciclin-like arabinogalactan protein
Potra2n15c28115	0.6	Potri.015G129400	FLA24		AT5G60490	FLA12	Fasciclin-like arabinogalactan protein
Potra2n9c19763	0.8	Potri.009G042500	LAC21	AA1	AT2G38080	LAC4/IRX12	Laccase
Potra2n6c14486	0.6	Potri.006G097100	LAC49	AA1	AT2G38080	LAC4/IRX12	Laccase
Potra2n6c14571	0.8	Potri.006G087500	LAC12	AA1	AT5G60020	LAC17	Laccase
Potra2n14c27476	1.1	Potri.012G042800	PRX67		AT2G39040	PER24	Class III peroxidase*****
Potra2n2c5834	−1.9	Potri.002G065300	PRX17		AT1G71695	PRX12	Class III peroxidase*****
Potra2n4c9733	−2.3	Potri.004G144600	PRX30		AT1G49570	PRX10	Class III peroxidase*****
Potra2n7c16468	−4.5	Potri.005G118700	PRX34		AT5G66390	PRX72	Class III peroxidase*****
Potra2n14c27252	1.0	Potri.014G113100			AT1G02520	ABCB11	ABC transporter
Potra2n9c19878	−1.5	Potri.009G028800		GH152	AT2G28790		Thaumatin family protein

**Populus tremula* v.2.2 gene ID.
**Best DIAMOND or phylogenetic tree-deduced assignment for homologous Potri gene ID based on Potra v.2.2 gene ID (for full annotation *cf* Supporting Information Tables S3 and S4).
***CAZy, carbohydrate-active enzyme family and gene name (Kumar *et al*., 2019).
****Best DIAMOND AGI gene ID based on Potra v.2.2 gene ID or phylogenetic tree-deduced assignment for homologous Ath based on Potri ID.
*****Populus* peroxidase names are according to Ren *et al*. (2014); FC, fold change (flexure/stationary expression).

© 2023 The Authors
New Phytologist © 2023 New Phytologist Foundation

14698137, 0, Downloaded from https://nph.onlinelibrary.wiley.com/doi/10.1111/nph.19307 by Swedish University Of Agricultural Sciences, Wiley Online Library on [15/11/2023]. See the Terms and Conditions (https://onlinelibrary.wiley.com/terms-and-conditions) on Wiley Online Library for rules of use; OA articles are governed by the applicable Creative Commons License

14698137, 0, Downloaded from https://nph.onlinelibrary.wiley.com/doi/10.1111/nph.19307 by Swedish University Of Agricultural Sciences, Wiley Online Library on [15/11/2023]. See the Terms and Conditions (https://onlinelibrary.wiley.com/terms-and-conditions) on Wiley Online Library for rules of use; OA articles are governed by the applicable Creative Commons License

Table 3 List of selected differentially expressed genes (DEGs; fold change ≥ 1.5) including Ca^{2+}-, G-protein- and receptor-like kinase-mediated signaling as well as hormone-related transcripts in the cambium and xylem tissues of mechanically stimulated hybrid aspen (*Populus tremula* × *tremuloides*) stems relative to the stationary set.

Potra v.2.2 gene ID*	Log_2 FC	Potri v.3.1 gene ID**	AGI gene ID***	AGI gene name (TAIR)	Description (TAIR, https://www.arabidopsis.org/)
Cambium					
Potra2n8c18019	0.9	Potri.008G151800	AT5G19530	ACL5	Thermospermine synthase
Potra2n1c2524	1.2	Potri.001G288900	AT1G10020		Formin-like protein (DUF1005)
Potra2n14c26822	0.7	Potri.014G066400	AT3G60550	CYP3;2	Cyclin p interacting with cyclin-dependent protein kinase
Potra2n12c24367	1.4	Potri.002G022500	AT5G14920	GASA14	Gibberellin-stimulated protein
Potra2n15c28577	0.9	Potri.T155100	AT5G14920	GASA14	Gibberellin-stimulated protein
Potra2n7c16398	0.8	Potri.005G124000	AT3G50660	DWF4/CYP90B1	C22 alpha hydroxylase
Potra2n7c15551	0.7	Potri.007G128600	AT2G43290	MSS3/CML5	Calmodulin-like protein
Potra2n1c3910	0.7	Potri.001G461400	AT1G30690	PATL4	Sec14p-like phosphatidylinositol transfer protein
Potra2n13c25391	0.6	Potri.019G079500	AT1G72160	PATL3	Sec14p-like phosphatidylinositol transfer protein
Potra2n1c3437	−1.7	Potri.011G112400	AT3G14440	NCED3	9-*cis*-epoxycarotenoid dioxygenase
Potra2n6c14762	−0.8	Potri.006G068500	AT5G25350	EBF2	EIN3-binding F-box protein
Potra2n18c32128	−0.9	Potri.018G130800	AT5G25350	EBF2	EIN3-binding F-box protein
Potra2n12c24080	−1.5	Potri.012G043200	AT1G73500	MKK9	Mitogen-activated protein kinase kinase
Potra2n16c30484	−1.5	Potri.016G134600	AT5G58350	WNK4	With no lysine (K) kinase
Potra2n8c17488	−1.5	Potri.008G096500	AT1G13740	AFP2	ABI five binding protein
Potra2n8c17832	−0.7	Potri.010G112200	AT3G18040	MPK9	Mitogen-activated protein kinase
Potra2n13c25835	−1.2	Potri.013G051300	AT5G63930		Leucine-rich repeat protein kinase
Potra2n15c28419	−1.2	Potri.015G086800	AT2G31880	SOBIR1	Leucine-rich repeat receptor-like kinase
Xylem					
Potra2n12c23757	0.7	Potri.012G007600	AT5G54130		Ca^{2+}-binding protein
Potra2n11c23262	0.7	Potri.011G063200	AT3G15050	IQD10	Calmodulin-binding protein
Potra2n16c29614	−3.1	Potri.006G046500	AT2G41560	ACA4	Calmodulin-regulated Ca^{2+}-ATPase
Potra2n2c4307	0.7	Potri.002G234600	AT3G07880	SCN1	RhoGTPase GDP dissociation inhibitor
Potra2n14c27583	0.6	Potri.014G147000	AT5G16490	RIC4	ROP-interactive CRIB motif-containing protein
Potra2n4c9197	0.6	Potri.004G086100	AT3G17840	RLK902	Receptor-like kinase
Potra2n2c4437	0.6	Potri.002G228200	AT1G05100	MAPKKK18	Mitogen-activated protein kinase kinase kinase
Potra2n14c27646	0.6	Potri.014G155000	AT1G05100	MAPKKK18	Mitogen-activated protein kinase kinase kinase
Potra2n7c16491	0.8	Potri.007G016800	AT5G66330		Leucine-rich repeat protein kinase
Potra2n2c5402	−2.5	Potri.002G111700	AT5G49660	XIP1/CEPR1	Leucine-rich repeat receptor kinase
Potra2n13c25987	1.8	Potri.013G035900	AT3G23750	BARK1/TMK4	Leucine-rich repeat receptor-like kinase
Potra2n6c14169	0.7	Potri.016G087800	AT3G53380	LECRK-VIII.1	L-type lectin receptor kinase
Potra2n8c17630	−2.0	Potri.008G110300	AT5G16000	NIK1	Leucine-rich repeat receptor-like kinase
Potra2n11c22876	−1.9	Potri.011G112400	AT3G14440	NCED3	9-*cis*-epoxycarotenoid dioxygenase
Potra2n1c3437	−1.9	Potri.011G112400	AT3G14440	NCED3	9-*cis*-epoxycarotenoid dioxygenase
Potra2n2c5263	0.9	Potri.002G126100	AT3G19270	CYP707A4	ABA 8′-hydroxylase
Potra2n14c27095	−0.8	Potri.014G095500	AT2G46370	JAR1	Jasmonate-amido synthetase
Potra2n10c21496	−0.7	Potri.010G108200	AT3G17860	JAZ3	Jasmonate-ZIM-domain protein 3
Potra2n747s36676	1.6	Potri.002G224100	AT1G05010	ACO4/EFE	ACC oxidase
Potra2n12c24119	−0.7	Potri.015G038700	AT1G73590	PIN1	Auxin efflux carrier
Potra2n2c5623	0.7	Potri.002G087000	AT1G77690	LAX3	Auxin influx carrier
Potra2n6c14477	−0.6	Potri.006G098300	AT2G38120	AUX1	Auxin influx carrier
Potra2n11c22589	0.8	Potri.001G458000	AT3G12955	SAUR74	SAUR-like auxin-responsive protein
Potra2n1c3857	0.7	Potri.001G458000	AT3G12955	SAUR74	SAUR-like auxin-responsive protein
Potra2n12c24367	1.5	Potri.002G022500	AT5G14920	GASA14	Gibberellin-stimulated protein
Potra2n14c27286	1.4	Potri.014G117300	AT1G02400	GA2OX6	Gibberellin 2-oxidase
Potra2n7c16146	−1.3	Potri.005G111700	AT2G17820	AHK1	Histidine kinase
Potra2n15c28548	−1.4	Potri.015G074600	AT5G13700	PAO1	Polyamine oxidase
Potra2n1022s36932	9.2	Potri.004G163300	AT2G16500	ADC1	Arginine decarboxylase
Potra2n5c11193	−1.3	Potri.005G185700	AT1G77000	SKP2B	Protein of E3 ubiquitin ligase SCF complex

**Populus tremula* genome assembly v.2.2 gene ID.
**Best DIAMOND Potri gene ID based on Potra v.2.2 gene ID.
***Best DIAMOND AGI gene ID based on Potra v.2.2 gene ID; FC, fold change (flexure/stationary expression).

relatively low (4°), compared with angles used in some other studies (30–45°) reporting inhibition of stem and leaf elongation (Pruyn *et al.*, 2000; Kern *et al.*, 2005). Our treatment also differed from plant rubbing used for herbaceous plants (Jaffe *et al.*, 1980; Saidi *et al.*, 2010; Chehab *et al.*, 2012) or stem bending as it was applied in the previous above-mentioned studies, since the stem in our

© 2023 The Authors
New Phytologist © 2023 New Phytologist Foundation

experiment was allowed to vibrate after each acceleration/deceleration (Video S1). Interestingly, sound vibrations have been shown to induce overall growth in many species (Jung *et al.*, 2018) and to induce responses at a distance (Appel & Cocroft, 2014).

Properties of flexure wood induced by low-intensity stem flexing

Detailed anatomical investigations revealed that flexed aspen formed significantly more secondary xylem compared with the stationary trees due to an increased number of xylem descendants of each fusiform initial (Fig. 2). This was supported by increased expression of cyclin *CYCP3*;2 in the cambium and decreased expression of the negative regulator of cell cycle *SKP2B* in the xylem (Table 3), suggesting that the population of dividing xylem mother cells was increased by mechanical stress. These data support and extend the conclusions from many other reports (Pruyn *et al.*, 2000; Kern *et al.*, 2005; Coutand *et al.*, 2008; Telewski, 2016; Roignant *et al.*, 2018).

Stem flexing also strongly affected xylem cell differentiation. The most striking change was the induction of G-fiber biosynthesis, resulting in overall phenotypical changes typical of tension wood (Fagerstedt *et al.*, 2014), such as decreased MFA and xylan content, increased cell wall thickness, wood density, fiber coarseness, nanoporosity, crystalline cellulose and galactan contents as well as yields of sugars from enzymatic saccharification of wood without pretreatment (Figs 2–4). Despite decreased xylan content, several genes encoding xylan acetyltransferases were upregulated in flexure wood (Table 2; Fig. S7), suggesting increased xylan acetylation, which would affect xylan interaction with cellulose (Grantham *et al.*, 2017) and lignin (Giummarella & Lawoko, 2016), and would thus mediate mechanical properties of flexure wood (Niez *et al.*, 2020).

Unilateral stem bending for 5 s also induced G-fibers but only on the tensile/upper side of the bent stems (Roignant *et al.*, 2018), indicating that G-fibers can be induced after much shorter stimulation times than previously anticipated (Jourez & Avella-Shaw, 2003; Coutand, 2010) and their molecular triggers could be similar for flexure and tension wood. Reports of reduced vessel frequency and diameter in poplar flexure wood (Kern *et al.*, 2005; Roignant *et al.*, 2018) and other hardwood species (Telewski, 2016) could also reflect activation of the tension wood program by stem bending, although we did not detect such changes in this study. Whether the triggers of flexure wood G-fibers respond to stem stretching or to gravity vector deflection, as in tension wood (Groover, 2016), remains to be established.

Flexure wood shares developmental program with tension wood but not with opposite wood

As each stem flexure induces tensional strain together with gravistimulation inducing tension wood and compression strain together with gravistimulation inducing opposite wood, the multiple flexures in different planes induce all these stresses alternately. To reveal the common response between flexure treatment and gravitationally induced tension and opposite wood, we compared the DEGs from our study with 8000 DEGs between tension and opposite wood in gravistimulated stems for different durations (2 h to 14 d; Zinkgraf *et al.*, 2018). Approximately 40% of flexure-affected genes were also differentially expressed between gravitropically induced tension and opposite wood (Tables S3, S4). Remarkably, almost all of them (97%) reacted the same way as in tension wood. This indicates that flexure wood shares the molecular program with gravitationally induced tension wood rather than opposite wood. Approximately 60% of DEGs in both cambium and xylem were not affected by gravitational stimuli and potentially reflect compression and/or tensional strain signaling. Interestingly, *KNAT3* and *MYB52* were among these genes and could regulate the secondary cell wall biosynthetic program contributing to decreased wall thickness in response to mechanical stress.

Membrane-attached proteins as putative mechanical stress sensors in flexure wood

Among different candidates for perception of mechanical disturbance (Fruleux *et al.*, 2019), we found several genes encoding proteins linking the cell wall with plasma membrane that were upregulated in flexure wood. *FLA11/FLA12s* are examples of such genes and were recently shown to control secondary cell wall thickening and lignification in Arabidopsis (Ma *et al.*, 2022). Other candidates are *XTHs* encoding XET, which are well-known touch- and bending-responsive genes (Lee *et al.*, 2005; Pomiès *et al.*, 2017). Some of the encoded XETs, including *Pt*XTH41 (*At*XTH30), have plasma membrane localization (Ndamukong *et al.*, 2009; Witasari *et al.*, 2019; Yan *et al.*, 2019); others could be associated with the plasma membrane via another XTH protein (Zhu *et al.*, 2014). Since the active site of XETs is covalently binding xyloglucan in cell walls, these proteins are good candidates for sensing mechanical stresses. In support, overexpression of *AtTCH4/XTH22* in Arabidopsis resulted in increased cell wall porosity (Zhang *et al.*, 2022), reminiscent of changes in flexure wood (Fig. 3d), whereas mutations in *xth4* and *xth9* resulted in changes in secondary cell wall layers and lignification with the activation of cell wall integrity-related genes (Kushwah *et al.*, 2020). Formins were also proposed as proteins involved in mechanical stress perception (Baluška *et al.*, 2003). How these plasma membrane-attached proteins could be involved in perception of mechanical stress is a matter of conjecture. The general belief is that they could provide a means for transferring mechanical strains of cell walls to the plasma membrane activating other sensors located there, such as stretch-activated ion channels, or that they could provide a physical link between the cell wall and actin filaments (with participation of other proteins) generating cell wall – plasma membrane – cytoskeleton continuity (Baluška *et al.*, 2003; Telewski, 2021).

Hormones involved in flexure wood formation

Our hormonomics and transcriptomics analyses provided evidence for the hormonal signaling during flexure wood formation, which is summarized in Fig. 7.

© 2023 The Authors
New Phytologist © 2023 New Phytologist Foundation

14698137, 0, Downloaded from https://nph.onlinelibrary.wiley.com/doi/10.1111/nph.19307 by Swedish University Of Agricultural Sciences, Wiley Online Library on [15/11/2023]. See the Terms and Conditions (https://onlinelibrary.wiley.com/terms-and-conditions) on Wiley Online Library for rules of use; OA articles are governed by the applicable Creative Commons License

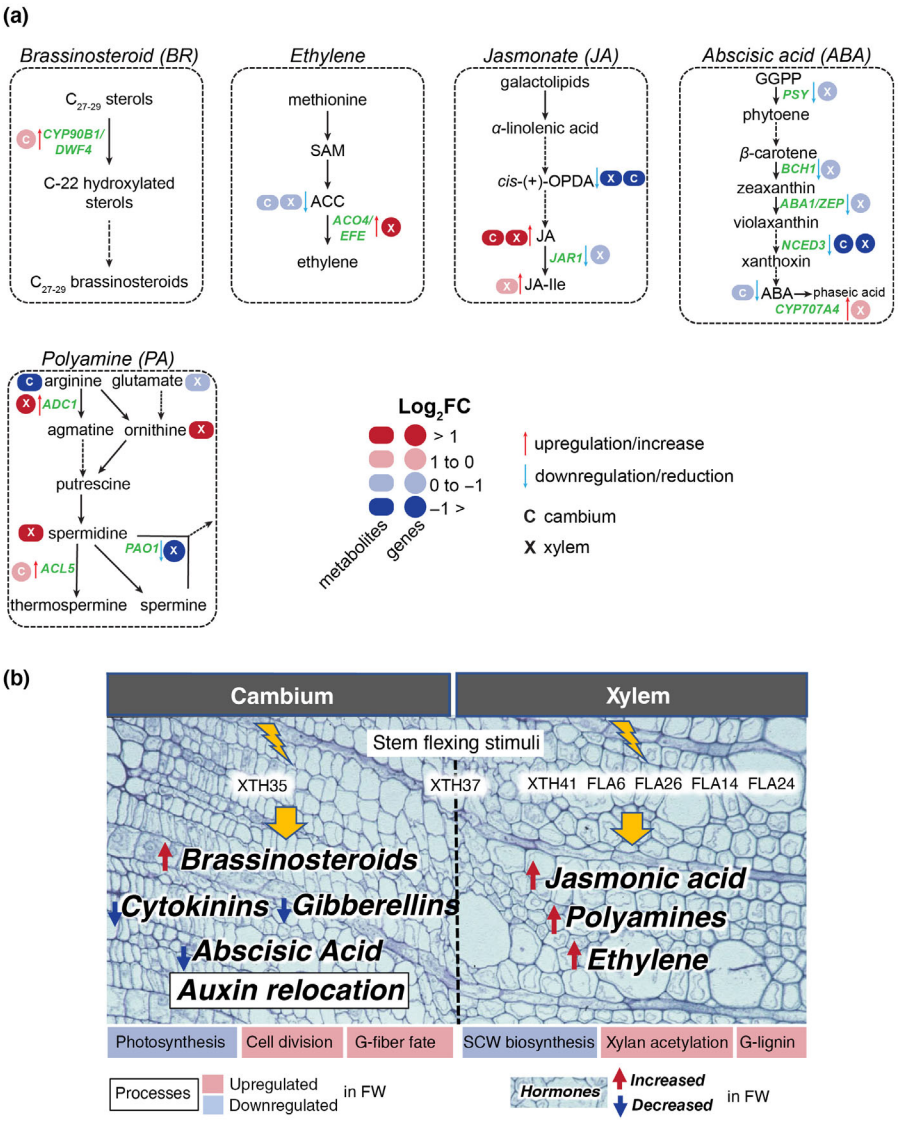

Fig. 7 Summary of main results from transcriptomics and hormonomics analyses in flexure wood highlighting main changes in hormones and processes affected in the cambium and xylem tissues of hybrid aspen (*Populus tremula* × *tremuloides*). (a) Changes in brassinosteroid, ethylene, jasmonates, abscisic acid and polyamine biosynthesis. Continuous arrows depict single enzymatic steps, whereas dashed arrows indicate the involvement of multiple enzymes and intermediates. Gene names are shown in green and are according to the *Arabidopsis* nomenclature. (b) Graphical summary highlighting main processes and hormonal changes identified in the cambial region tissues (cambium) and developing xylem (xylem) tissues. The background micrograph represents the analyzed tissues. Proteins listed in the upper part of the diagram represent main candidates for the perception of mechanical stimuli identified by transcriptomics. Red boxes, circles, ovals and arrows indicate upregulated processes, genes, metabolites and hormonal pathways/signaling; blue boxes, circles, ovals and arrows indicate downregulated processes, genes, metabolites and hormonal pathways/signaling. FW, flexure wood.

Prominent changes in PA metabolism are indicative of increased levels of PA signaling during flexure wood formation, which have not been previously observed in gravitropically or mechanically stimulated plants. Our findings, along with the report in Chinese cabbage on increased PAs in plants exposed to sound vibration (Qin *et al.*, 2003), suggest that PAs could be involved in mechanoresponses.

The substantial changes in jasmonate levels observed in flexed stems (Fig. 7) mimic those in mechanostimulated Arabidopsis leaves (Chehab *et al.*, 2012) and could be responsible for increased xylem production (Sehr *et al.*, 2010). These prominent metabolic changes in developing flexure wood were not reflected in transcriptomes (Table 3). The jasmonate-related genes are considered as early touch-responsive genes (Van Moerkercke *et al.*, 2019). They were shown to be upregulated only shortly after a single stem bending in poplar but not after subsequent bending (Pomiès *et al.*, 2017). Thus, the jasmonate-related transcriptome could be dampened upon repetitive mechanostimulations during flexure wood formation, as was observed for other touch genes in poplar stems subjected to repetitive bending (Martin *et al.*, 2010).

There was a coordinate downregulation of the ABA biosynthetic pathway along with decreased ABA levels during the flexure wood response (Fig. 7). Decreased ABA was reported in different mechanically stressed plants (Ishihara *et al.*, 2017; Van Moerkercke *et al.*, 2019; Li *et al.*, 2023), suggesting that it might be a general mechanical stress response. Catabolism of GA also appears to be similar between flexure wood and touch response, with common upregulation of *GA2OX6* (Table 3; Lange & Lange, 2015). Although GAs are positive regulators of tension wood (Funada *et al.*, 2008; Gerttula *et al.*, 2015; Wang *et al.*, 2017), our findings suggest that this pathway is not used for G-fiber induction in flexure wood. By contrast, we find support for the involvement of ethylene in flexure wood, which could be responsible for G-fiber induction and increased growth, similar to its role in tension wood (Andersson-Gunnerås

© 2023 The Authors
New Phytologist © 2023 New Phytologist Foundation

14698137, 0, Downloaded from https://nph.onlinelibrary.wiley.com/doi/10.1111/nph.19307 by Swedish University Of Agricultural Sciences, Wiley Online Library on [15/11/2023]. See the Terms and Conditions (https://onlinelibrary.wiley.com/terms-and-conditions) on Wiley Online Library for rules of use; OA articles are governed by the applicable Creative Commons License

et al., 2006; Love *et al.*, 2009; Felten *et al.*, 2018). Ethylene signaling is also involved in thigmomorphogenesis in other plant species that do not form G-fibers (Telewski, 2021; Brenya *et al.*, 2022). Our transcriptome data provide some evidence for involvement of BRs during flexure wood induction (Table 3; Fig. 7), in agreement with their positive role in xylem proliferation and G-fiber production (Du *et al.*, 2020; Jin *et al.*, 2020). The BRs are part of early touch responses along with jasmonates, ethylene and auxins (Brenya *et al.*, 2022). In flexure wood, there was indication of a change in auxin transport, which is a key response during gravitropically induced tension wood (Gerttula *et al.*, 2015), based on altered expression of different auxin transporters (Table 3). Thus, this analysis of flexure wood formation in aspen supports a novel involvement of PAs, as well as involvement of jasmonate, ethylene, BR, ABA, GA and auxin signaling, which are also known to be implicated in other mechanoresponses of plants.

In conclusion, this study provides evidence of overall growth stimulation in aspen subjected to multidirectional low-intensity stem flexures, and the formation of flexure wood that exhibited altered cell wall structure, composition and nanoporosity, resulting in improved saccharification properties. The transcriptional program of flexure wood partially overlapped the tension wood program but not the opposite wood program. Induction of different membrane-attached proteins that could be connected to cell wall components, such as FLAs and XTHs, supports the idea that they could act as mechanosensors of flexure wood (Fig. 7b). Changes in transcripts and hormone levels in the cambium and developing xylem of flexed trees provided evidence for increased PAs, JA ethylene, auxin and BR signaling, and decreased ABA and GA signaling in flexure wood formation. Many of these pathways are also known to be involved in thigmomorphogenesis in other plant tissues and some are shared with tension wood responses. These findings contribute to the emerging picture of transcriptional and hormonal control of flexure and tension wood formation in poplar (Gerttula *et al.*, 2015; Pomiès *et al.*, 2017; Zinkgraf *et al.*, 2018; Lopez *et al.*, 2021), improving our understanding on how gravitational and/or mechanical stimulation influence secondary growth in woody species.

Acknowledgements

We acknowledge the Bioinformatics Facility at UPSC for bioinformatic analyses, Dr Junko Takahashi-Schmidt and the Biopolymer Analytical Platform (BAP) at UPSC for the help with cell wall chemistry analyses, the UPSC Microscopy Facility for help with wood anatomy analyses and the Swedish Metabolomics Centre in Umeå for carrying out metabolite analyses. The work was funded by the Knut and Alice Wallenberg (KAW) Foundation, VR, Bio4Energy and T4F programs. M.K. was supported by a junior grant (20-25948Y) from the Czech Science Foundation (GAČR).

Competing interests

None declared.

Author contributions

JU analyzed the data and wrote the manuscript. END performed growth phenotyping and RNA analyses and analyzed transcriptomics data. PS analyzed wood chemical composition and carried out light microscopy analyses. EvZ, ND and NRS carried out comparative transcriptome analyses. FRB and MD-M helped with setting up the experiment. JŠ, MK and KL analyzed hormones. ZY and GS carried out wood SilviScan analyses. MLG, SW and LJJ analyzed saccharification potential, microporosity and cellulose content. EJM designed and coordinated experimental work and finalized the manuscript with contributions from all authors. JU and END contributed equally to this work.

ORCID

Félix R. Barbut https://orcid.org/0000-0001-5395-6776
Nicolas Delhomme https://orcid.org/0000-0002-3053-0796
Marta Derba-Maceluch https://orcid.org/0000-0002-8034-3630
Evgeniy N. Donev https://orcid.org/0000-0002-7279-0481
Madhavi L. Gandla https://orcid.org/0000-0003-2798-6298
Leif J. Jönsson https://orcid.org/0000-0003-3866-0111
Michal Karady https://orcid.org/0000-0002-5603-706X
Karin Ljung https://orcid.org/0000-0003-2901-189X
Ewa J. Mellerowicz https://orcid.org/0000-0001-6817-1031
Gerhard Scheepers https://orcid.org/0000-0002-5630-1377
Jan Šimura https://orcid.org/0000-0002-1567-2278
Pramod Sivan https://orcid.org/0000-0001-5297-2221
Nathaniel R. Street https://orcid.org/0000-0001-6031-005X
János Urbancsok https://orcid.org/0000-0003-3237-6806
Sandra Winestrand https://orcid.org/0000-0001-8784-9696
Zakiya Yassin https://orcid.org/0000-0001-6878-3361
Elena van Zalen https://orcid.org/0000-0003-1621-3222

Data availability

The raw RNA-Seq data that support the findings of this study are openly available in the European Nucleotide Archive (ENA) at EMBL-EBI (https://www.ebi.ac.uk/ena/browser/home), under accession no. PRJEB61635.

References

Alonso-Serra J, Shi X, Peaucelle A, Rastas P, Bourdon M, Immanen J, Takahashi J, Koivula H, Eswaran G, Muranen S *et al.* 2020. *ELIMÄKI* locus is required for vertical proprioceptive response in birch trees. *Current Biology* **30**: 589–599.

Andersson-Gunnerås S, Mellerowicz EJ, Love J, Segerman B, Ohmiya Y, Coutinho PM, Nilsson P, Henrissat B, Moritz T, Sundberg B. 2006. Biosynthesis of cellulose-enriched tension wood in *Populus*: global analysis of transcripts and metabolites identifies biochemical and developmental regulators in secondary wall biosynthesis. *The Plant Journal* **45**: 144–165.

Appel HM, Cocroft RB. 2014. Plants respond to leaf vibrations caused by insect herbivore chewing. *Oecologia* **175**: 1257–1266.

Arnaud D, Déjardin A, Leplé J-C, Lesage-Descauses M-C, Pilate G. 2007. Genome-wide analysis of LIM gene family in *Populus trichocarpa*, *Arabidopsis thaliana*, and *Oryza sativa*. *DNA Research* **14**: 103–116.

© 2023 The Authors
New Phytologist © 2023 New Phytologist Foundation

14698137, 0, Downloaded from https://nph.onlinelibrary.wiley.com/doi/10.1111/nph.19307 by Swedish University Of Agricultural Sciences, Wiley Online Library on [15/11/2023]. See the Terms and Conditions (https://onlinelibrary.wiley.com/terms-and-conditions) on Wiley Online Library for rules of use; OA articles are governed by the applicable Creative Commons License

Bacete L, Hamann T. 2020. The role of mechanoperception in plant cell wall integrity maintenance. *Plants* **9**: 574.

Baluška F, Šamaj J, Wojtaszek P, Volkmann D, Menzel D. 2003. Cytoskeleton-plasma membrane-cell wall continuum in plants. Emerging links revisited. *Plant Physiology* **133**: 483–491.

Basu D, Haswell ES. 2017. Plant mechanosensitive ion channels: an ocean of possibilities. *Current Opinion in Plant Biology* **40**: 43–48.

Benikhlef L, L'Haridon F, Abou-Mansour E, Serrano M, Binda M, Costa A, Lehmann S, Métraux J-P. 2013. Perception of soft mechanical stress in *Arabidopsis* leaves activates disease resistance. *BMC Plant Biology* **13**: 133.

Berthet S, Demont-Caulet N, Pollet B, Bidzinski P, Cézard L, Le Bris P, Borrega N, Hervé J, Blondet E, Balzergue S *et al.* 2011. Disruption of LACCASE4 and 17 results in tissue-specific alterations to lignification of *Arabidopsis thaliana* stems. *Plant Cell* **23**: 1124–1137.

Braam J. 2005. In touch: plant responses to mechanical stimuli. *New Phytologist* **165**: 373–389.

Braam J, Davis RW. 1990. Rain-, wind- and touch-induced expression of calmodulin and calmodulin-related genes in Arabidopsis. *Cell* **60**: 357–364.

Brenya E, Chen Z-H, Tissue D, Papanicolaou A, Cazzonelli CI. 2020. Prior exposure of *Arabidopsis* seedlings to mechanical stress heightens jasmonic acid-mediated defense against necrotrophic pathogens. *BMC Plant Biology* **20**: 548.

Brenya E, Pervin M, Chen ZH, Tissue DT, Johnson S, Braam J, Cazzonelli CI. 2022. Mechanical stress acclimation in plants: linking hormones and somatic memory to thigmomorphogenesis. *Plant, Cell & Environment* **45**: 989–1010.

Brunauer S, Emmett PH, Teller E. 1938. Adsorption of gases in multimolecular layers. *Journal of the American Chemical Society* **60**: 309–319.

Bryan AC, Obaidi A, Wierzba M, Tax FE. 2012. XYLEM INTERMIXED WITH PHLOEM1, a leucine-rich repeat receptor-like kinase required for stem growth and vascular development in *Arabidopsis thaliana*. *Planta* **235**: 111–122.

Cassan-Wang H, Goué N, Saidi M, Legay S, Sivadon P, Goffner D, Grima-Pettenati J. 2013. Identification of novel transcription factors regulating secondary cell wall formation in *Arabidopsis*. *Frontiers in Plant Science* **4**: 189.

Chai G, Kong Y, Zhu M, Yu L, Qi G, Tang X, Wang Z, Cao Y, Yu C, Zhou G. 2015. *Arabidopsis* C3H14 and C3H15 have overlapping roles in the regulation of secondary wall thickening and anther development. *Journal of Experimental Botany* **66**: 2595–2609.

Chang S, Puryear J, Cairney J. 1993. A simple and efficient method for isolating RNA from pine trees. *Plant Molecular Biology Reporter* **11**: 113–116.

Chehab EW, Eich E, Braam J. 2009. Thigmomorphogenesis: a complex plant response to mechano-stimulation. *Journal of Experimental Botany* **60**: 43–56.

Chehab EW, Yao C, Henderson Z, Kim S, Braam J. 2012. *Arabidopsis* touch-induced morphogenesis is jasmonate mediated and protects against pests. *Current Biology* **22**: 701–706.

Chong S-L, Koutaniemi S, Virkki L, Pynnönen H, Tuomainen P, Tenkanen M. 2013. Quantitation of 4-*O*-methylglucuronic acid from plant cell walls. *Carbohydrate Polymers* **91**: 626–630.

Coutand C. 2010. Mechanosensing and thigmomorphogenesis, a physiological and biomechanical point of view. *Plant Science* **179**: 168–182.Coutand C, Julien JL, Moulia B, Mauget JC, Guitard D. 2000. Biomechanical study of the effect of a controlled bending on tomato stem elongation: global mechanical analysis. J Exp Bot. 51:1813-24.

Coutand C, Dupraz C, Jaouen G, Ploquin S, Adam B. 2008. Mechanical stimuli regulate the allocation of biomass in trees: demonstration with young *Prunus avium* trees. *Annals of Botany* **101**: 1421–1432.

Coutand C, Julien JL, Moulia B, Mauget JC, Guitard D. 2000. Biomechanical study of the effect of a controlled bending on tomato stem elongation: global mechanical analysis. *Journal of Experimental Botany* **51**: 1813–1824.

Coutand C, Martin L, Leblanc-Fournier N, Decourteix ML, Julien J-L, Moulia B. 2009. Strain mechanosensing quantitatively controls diameter growth and *PtaZFP2* gene expression in poplar. *Plant Physiology* **151**: 223–232.

Desprez T, Juraniec M, Crowell EF, Jouy H, Pochylova Z, Parcy F, Höfte H, Gonneau M, Vernhettes S. 2007. Organization of cellulose synthase complexes involved in primary cell wall synthesis in *Arabidopsis thaliana*. *Proceedings of the National Academy of Sciences, USA* **104**: 15572–15577.

Du J, Gerttula S, Li Z, Zhao S-T, Liu Y-L, Liu Y, Lu M-Z, Groover AT. 2020. Brassinosteroid regulation of wood formation in poplar. *New Phytologist* **225**: 1516–1530.

Evans R, Ilic J. 2001. Rapid prediction of wood stiffness from microfibril angle and density. *Forest Products Journal* **51**: 53–57.

Evans R, Stuart SA, Van Der Touw J. 1996. Microfibril angle scanning of increment cores by X-ray densitometry. *Appita Journal* **49**: 411–414.

Fagerstedt KV, Mellerowicz E, Gorshkova T, Ruel K, Joseleau J-P. 2014. Cell wall polymers in reaction wood. In: Gardiner B, Barnett J, Saranpää P, Gril J, eds. *The biology of reaction wood*. Berlin, Germany: Springer, 37–106.

Felten J, Vahala J, Love J, Gorzsás A, Rüggeberg M, Delhomme N, Leśniewska J, Kangasjärvi J, Hvidsten TR, Mellerowicz EJ *et al.* 2018. Ethylene signaling induces gelatinous layers with typical features of tension wood in hybrid aspen. *New Phytologist* **218**: 999–1014.

Fernández-Pérez F, Pomar F, Pedreño MA, Novo-Uzal E. 2015. Suppression of *Arabidopsis* peroxidase 72 alters cell wall and phenylpropanoid metabolism. *Plant Science* **239**: 192–199.

Franke R, Humphreys JM, Hemm MR, Denault JW, Ruegger MO, Cusumano JC, Chapple C. 2002. The *Arabidopsis* REF8 gene encodes the 3-hydroxylase of phenylpropanoid metabolism. *The Plant Journal* **30**: 33–45.

Fruleux A, Verger S, Boudaoud A. 2019. Feeling stressed or strained? A biophysical model for cell wall mechanosensing in plants. *Frontiers in Plant Science* **10**: 757.

Fujita S, Ohnishi T, Watanabe B, Yokota T, Takatsuto S, Fujioka S, Yoshida S, Sakata K, Mizutani M. 2006. *Arabidopsis* CYP90B1 catalyses the early C-22 hydroxylation of C27, C28 and C29 sterols. *The Plant Journal* **45**: 765–774.

Funada R, Miura T, Shimizu Y, Kinase T, Nakaba S, Kubo T, Sano Y. 2008. Gibberellin-induced formation of tension wood in angiosperm trees. *Planta* **227**: 1409–1414.

Gandla ML, Derba-Maceluch M, Liu X, Gerber L, Master ER, Mellerowicz EJ, Jönsson LJ. 2015. Expression of a fungal glucuronoyl esterase in *Populus*: effects on wood properties and saccharification efficiency. *Phytochemistry* **112**: 210–220.

Gandla ML, Mähler N, Escamez S, Skotare T, Obudulu O, Möller L, Abreu IN, Bygdell J, Hertzberg M, Hvidsten TR *et al.* 2021. Overexpression of vesicle-associated membrane protein PttVAP27-17 as a tool to improve biomass production and the overall saccharification yields in *Populus* trees. *Biotechnology for Biofuels* **14**: 43.

Gartner BL. 1994. Root biomechanics and whole-plant allocation patterns: responses of tomato plants to stem flexure. *Journal of Experimental Botany* **45**: 1647–1654.

Gerber L, Eliasson M, Trygg J, Moritz T, Sundberg B. 2012. Multivariate curve resolution provides a high-throughput data processing pipeline for pyrolysis-gas chromatography/mass spectrometry. *Journal of Analytical and Applied Pyrolysis* **95**: 95–100.

Gerttula S, Zinkgraf M, Muday GK, Lewis DR, Ibatullin FM, Brumer H, Hart F, Mansfield SD, Filkov V, Groover A. 2015. Transcriptional and hormonal regulation of gravitropism of woody stems in *Populus*. *Plant Cell* **27**: 2800–2813.

Ghosh R, Barbacci A, Leblanc-Fournier N. 2021. Mechanostimulation: a promising alternative for sustainable agriculture practices. *Journal of Experimental Botany* **72**: 2877–2888.

Giummarella N, Lawoko M. 2016. Structural basis for the formation and regulation of lignin–xylan bonds in birch. *ACS Sustainable Chemistry & Engineering* **4**: 5319–5326.

Grantham NJ, Wurman-Rodrich J, Terrett OM, Lyczakowski JJ, Stott K, Iuga D, Simmons TJ, Durand-Tardif M, Brown SP, Dupree R *et al.* 2017. An even pattern of xylan substitution is critical for interaction with cellulose in plant cell walls. *Nature Plants* **3**: 859–865.

Groover A. 2016. Gravitropisms and reaction woods of forest trees – evolution, functions and mechanisms. *New Phytologist* **211**: 790–802.

Gu Z, Eils R, Schlesner M. 2016. Complex heatmaps reveal patterns and correlations in multidimensional genomic data. *Bioinformatics* **32**: 2847–2849.

Heinemann KJ, Yang S-Y, Straube H, Medina-Escobar N, Varbanova-Herde M, Herde M, Rhee S, Witte C-P. 2021. Initiation of cytosolic plant purine

© 2023 The Authors
New Phytologist © 2023 New Phytologist Foundation

14698137, 0, Downloaded from https://nph.onlinelibrary.wiley.com/doi/10.1111/nph.19307 by Swedish University Of Agricultural Sciences, Wiley Online Library on [15/11/2023]. See the Terms and Conditions (https://onlinelibrary.wiley.com/terms-and-conditions) on Wiley Online Library for rules of use; OA articles are governed by the applicable Creative Commons License

nucleotide catabolism involves a monospecific xanthosine monophosphate phosphatase. *Nature Communications* **12**: 6846.

Hoffmann N, Benske A, Betz H, Schuetz M, Samuels AL. 2020. Laccases and peroxidases co-localize in lignified secondary cell walls throughout stem development. *Plant Physiology* **184**: 806–822.

Hu H, Zhang R, Feng S, Wang Y, Wang Y, Fan C, Li Y, Liu Z, Schneider R, Xia T *et al.* 2018. Three AtCesA6-like members enhance biomass production by distinctively promoting cell growth in *Arabidopsis*. *Plant Biotechnology Journal* **16**: 976–988.

Ishihara KL, Lee EKW, Borthakur D. 2017. Thigmomorphogenesis: changes in morphology, biochemistry, and levels of transcription in response to mechanical stress in *Acacia koa*. *Canadian Journal of Forest Research* **47**: 583–593.

Iuchi S, Kobayashi M, Taji T, Naramoto M, Seki M, Kato T, Tabata S, Kakubari Y, Yamaguchi-Shinozaki K, Shinozaki K. 2001. Regulation of drought tolerance by gene manipulation of 9-cis-epoxycarotenoid dioxygenase, a key enzyme in abscisic acid biosynthesis in *Arabidopsis*. *The Plant Journal* **27**: 325–333.

Jaffe MJ. 1973. Thigmomorphogenesis: the response of plant growth and development to mechanical stimulation. *Planta* **114**: 143–157.

Jaffe MJ, Biro R, Bridle K. 1980. Thigmomorphogenesis: calibration of the parameters of the sensory function in beans. *Physiologia Plantarum* **49**: 410–416.

Jiang H, Tang B, Xie Z, Nolan T, Ye H, Song G-Y, Walley J, Yin Y. 2019. GSK3-like kinase BIN2 phosphorylates RD26 to potentiate drought signaling in *Arabidopsis*. *The Plant Journal* **100**: 923–937.

Jin Y, Yu C, Jiang C, Guo X, Li B, Wang C, Kong F, Zhang H, Wang H. 2020. *PtiCYP85A3*, a BR C-6 oxidase gene, plays a critical role in brassinosteroid-mediated tension wood formation in poplar. *Frontiers in Plant Science* **11**: 468.

Jourez B, Avella-Shaw T. 2003. Effet de la durée d'application d'un stimulus gravitationnel sur la formation de bois de tension et de bois opposé dans de jeunes pousses de peuplier (*Populus euramericana* cv 'Ghoy'). *Annals of Forest Science* **60**: 31–41.

Jung J, Kim S-K, Kim JY, Jeong M-J, Ryu C-M. 2018. Beyond chemical triggers: evidence for sound-evoked physiological reactions in plants. *Frontiers in Plant Science* **9**: 25.

Kaida R, Sasaki Y, Ozaki K, Ki B, Momoi T, Ohbayashi H, Taji T, Sakata Y, Hayashi T. 2020. Intake of radionuclides in the trees of Fukushima forests 5. Earthquake could have caused an increase in xyloglucan in trees. *Forests* **11**: 966.

Kakehi J-I, Kuwashiro Y, Niitsu M, Takahashi T. 2008. Thermospermine is required for stem elongation in *Arabidopsis thaliana*. *Plant and Cell Physiology* **49**: 1342–1349.

Kaneda M, Schuetz M, Lin BSP, Chanis C, Hamberger B, Western TL, Ehlting J, Samuels AL. 2011. ABC transporters coordinately expressed during lignification of *Arabidopsis* stems include a set of ABCBs associated with auxin transport. *Journal of Experimental Botany* **62**: 2063–2077.

Kern KA, Ewers FW, Telewski FW, Koehler L. 2005. Mechanical perturbation affects conductivity, mechanical properties and aboveground biomass of hybrid poplars. *Tree Physiology* **25**: 1243–1251.

Kim D, Cho Y-h, Ryu H, Kim Y, Kim T-H, Hwang I. 2013. BLH1 and KNAT3 modulate ABA responses during germination and early seedling development in *Arabidopsis*. *The Plant Journal* **75**: 755–766.

Kumar M, Thammannagowda S, Bulone V, Chiang V, Han K-H, Joshi CP, Mansfield SD, Mellerowicz E, Sundberg B, Teeri T *et al.* 2009. An update on the nomenclature for the cellulose synthase genes in *Populus*. *Trends in Plant Science* **14**: 248–254.

Kumar V, Hainaut M, Delhomme N, Mannapperuma C, Immerzeel P, Street NR, Henrissat B, Mellerowicz EJ. 2019. Poplar carbohydrate-active enzymes: whole-genome annotation and functional analyses based on RNA expression data. *The Plant Journal* **99**: 589–609.

Kushiro T, Okamoto M, Nakabayashi K, Yamagishi K, Kitamura S, Asami T, Hirai N, Koshiba T, Kamiya Y, Nambara E. 2004. The *Arabidopsis* cytochrome P450 CYP707A encodes ABA 8′-hydroxylases: key enzymes in ABA catabolism. *EMBO Journal* **23**: 1647–1656.

Kushwah S, Banasiak A, Nishikubo N, Derba-Maceluch M, Majda M, Endo S, Kumar V, Gomez L, Gorzsas A, McQueen-Mason S *et al.* 2020. *Arabidopsis XTH4* and *XTH9* contribute to wood cell expansion and secondary wall formation. *Plant Physiology* **182**: 1946–1965.

Lafarguette F, Leplé J-C, Déjardin A, Laurans F, Costa G, Lesage-Descauses M-C, Pilate G. 2004. Poplar genes encoding fasciclin-like arabinogalactan proteins are highly expressed in tension wood. *New Phytologist* **164**: 107–121.

Lange MJP, Lange T. 2015. Touch-induced changes in *Arabidopsis* morphology dependent on gibberellin breakdown. *Nature Plants* **1**: 14025.

Leblanc-Fournier N, Coutand C, Crouzet J, Brunel N, Lenne C, Moulia B, Julien J-L. 2008. *Jr-ZFP2*, encoding a Cys2/His2-type transcription factor, is involved in the early stages of the mechano-perception pathway and specifically expressed in mechanically stimulated tissues in woody plants. *Plant, Cell & Environment* **31**: 715–726.

Lee C, Teng Q, Huang W, Zhong R, Ye Z-H. 2009. The poplar GT8E and GT8F glycosyltransferases are functional orthologs of *Arabidopsis* PARVUS involved in glucuronoxylan biosynthesis. *Plant and Cell Physiology* **50**: 1982–1987.

Lee C, Zhong R, Richardson EA, Himmelsbach DS, McPhail BT, Ye Z-H. 2007. The *PARVUS* Gene is expressed in cells undergoing secondary wall thickening and is essential for glucuronoxylan biosynthesis. *Plant and Cell Physiology* **48**: 1659–1672.

Lee D, Polisensky DH, Braam J. 2005. Genome-wide identification of touch- and darkness-regulated *Arabidopsis* genes: a focus on calmodulin-like and XTH genes. *New Phytologist* **165**: 429–444.

Li Q, Zargar O, Park S, Pharr M, Muliana A, Finlayson SA. 2023. Mechanical stimulation reprograms the sorghum internode transcriptome and broadly alters hormone homeostasis. *Plant Science* **327**: 111555.

Li W, Ma M, Feng Y, Li H, Wang Y, Ma Y, Li M, An F, Guo H. 2015. EIN2-directed translational regulation of ethylene signaling in *Arabidopsis*. *Cell* **163**: 670–683.

Lin C-Y, Li Q, Tunlaya-Anukit S, Shi R, Sun Y-H, Wang JP, Liu J, Loziuk P, Edmunds CW, Miller ZD *et al.* 2016. A cell wall-bound anionic peroxidase, PtrPO21, is involved in lignin polymerization in *Populus trichocarpa*. *Tree Genetics & Genomes* **12**: 22.

Liu B, Seong K, Pang S, Song J, Gao H, Wang C, Zhai J, Zhang Y, Gao S, Li X *et al.* 2021. Functional specificity, diversity, and redundancy of *Arabidopsis* JAZ family repressors in jasmonate and COI1-regulated growth, development, and defense. *New Phytologist* **231**: 1525–1545.

Lopez D, Franchel J, Venisse J-S, Drevet JR, Label P, Coutand C, Roeckel-Drevet P. 2021. Early transcriptional response to gravistimulation in poplar without phototropic confounding factors. *AoB Plants* **13**: plaa071.

Love J, Björklund S, Vahala J, Hertzberg M, Kangasjärvi J, Sundberg B. 2009. Ethylene is an endogenous stimulator of cell division in the cambial meristem of *Populus*. *Proceedings of the National Academy of Sciences, USA* **106**: 5984–5989.

Lu S, Li Q, Wei H, Chang M-J, Tunlaya-Anukit S, Kim H, Liu J, Song J, Sun Y-H, Yuan L *et al.* 2013. Ptr-miR397a is a negative regulator of laccase genes affecting lignin content in *Populus trichocarpa*. *Proceedings of the National Academy of Sciences, USA* **110**: 10848–10853.

Ma Y, MacMillan CP, de Vries L, Mansfield SD, Hao P, Ratcliffe J, Bacic A, Johnson KL. 2022. FLA11 and FLA12 glycoproteins fine-tune stem secondary wall properties in response to mechanical stresses. *New Phytologist* **233**: 1750–1767.

Manzano C, Ramirez-Parra E, Casimiro I, Otero S, Desvoyes B, De Rybel B, Beeckman T, Casero P, Gutierrez C, del Pozo JC. 2012. Auxin and epigenetic regulation of SKP2B, an F-box that represses lateral root formation. *Plant Physiology* **160**: 749–762.

Martin L, Decourteix M, Badel E, Huguet S, Moulia B, Julien J-L, Leblanc-Fournier N. 2014. The zinc finger protein PtaZFP2 negatively controls stem growth and gene expression responsiveness to external mechanical loads in poplar. *New Phytologist* **203**: 168–181.

Martin L, Leblanc-Fournier N, Azri W, Lenne C, Henry C, Coutand C, Julien J-L. 2009. Characterization and expression analysis under bending and other abiotic factors of PtaZFP2, a poplar gene encoding a Cys2/His2 zinc finger protein. *Tree Physiology* **29**: 125–136.

Martin L, Leblanc-Fournier N, Julien J-L, Moulia B, Coutand C. 2010. Acclimation kinetics of physiological and molecular responses of plants to multiple mechanical loadings. *Journal of Experimental Botany* **61**: 2403–2412.

© 2023 The Authors
New Phytologist © 2023 New Phytologist Foundation

14698137, 0, Downloaded from https://nph.onlinelibrary.wiley.com/doi/10.1111/nph.19307 by Swedish University Of Agricultural Sciences, Wiley Online Library on [15/11/2023]. See the Terms and Conditions (https://onlinelibrary.wiley.com/terms-and-conditions) on Wiley Online Library for rules of use; OA articles are governed by the applicable Creative Commons License

Monshausen GB, Haswell ES. 2013. A force of nature: molecular mechanisms of mechanoperception in plants. *Journal of Experimental Botany* **64**: 4663–4680.

Moulia B, Douady S, Hamant O. 2021. Fluctuations shape plants through proprioception. *Science* **372**: eabc6868.

Muñiz L, Minguet EG, Singh SK, Pesquet E, Vera-Sirera F, Moreau-Courtois CL, Carbonell J, Blázquez MA, Tuominen H. 2008. ACAULIS5 controls *Arabidopsis* xylem specification through the prevention of premature cell death. *Development* **135**: 2573–2582.

Nakagawa Y, Katagiri T, Shinozaki K, Qi Z, Tatsumi H, Furuichi T, Kishigami A, Sokabe M, Kojima I, Sato S *et al.* 2007. *Arabidopsis* plasma membrane protein crucial for Ca^{2+} influx and touch sensing in roots. *Proceedings of the National Academy of Sciences, USA* **104**: 3639–3644.

Ndamukong I, Chetram A, Saleh A, Avramova Z. 2009. Wall-modifying genes regulated by the *Arabidopsis* homolog of trithorax, ATX1: repression of the *XTH33* gene as a test case. *The Plant Journal* **58**: 541–553.

Niez B, Dlouha J, Gril J, Ruelle J, Toussaint E, Moulia B, Badel E. 2020. Mechanical properties of "flexure wood": compressive stresses in living trees improve the mechanical resilience of wood and its resistance to damage. *Annals of Forest Science* **77**: 17.

Paul-Victor C, Rowe N. 2011. Effect of mechanical perturbation on the biomechanics, primary growth and secondary tissue development of inflorescence stems of *Arabidopsis thaliana*. *Annals of Botany* **107**: 209–218.

Pomiès L, Decourteix M, Franchel J, Moulia B, Leblanc-Fournier N. 2017. Poplar stem transcriptome is massively remodelled in response to single or repeated mechanical stimuli. *BMC Genomics* **18**: 300.

Pramod S, Gandla ML, Derba-Maceluch M, Jönsson LJ, Mellerowicz EJ, Winestrand S. 2021. Saccharification potential of transgenic greenhouse- and field-grown aspen engineered for reduced xylan acetylation. *Frontiers in Plant Science* **12**: 704960.

Pruyn ML, Ewers BJ III, Telewski FW. 2000. Thigmomorphogenesis: changes in the morphology and mechanical properties of two *Populus* hybrids in response to mechanical perturbation. *Tree Physiology* **20**: 535–540.

Qin Y-C, Lee W-C, Choi Y-C, Kim T-W. 2003. Biochemical and physiological changes in plants as a result of different sonic exposures. *Ultrasonics* **41**: 407–411.

R Core Team. 2022. *R: A language and environment for statistical computing.* Vienna, Austria: R Foundation for Statistical Computing. [WWW document] URL https://www.R-project.org [accessed 10 October 2023].

Rajangam AS, Kumar M, Aspeborg H, Guerriero G, Arvestad L, Pansri P, Brown CJ-L, Hober S, Blomqvist K, Divne C *et al.* 2008. MAP20, a microtubule-associated protein in the secondary cell walls of hybrid aspen, is a target of the cellulose synthesis inhibitor 2,6-dichlorobenzonitrile. *Plant Physiology* **148**: 1283–1294.

Ren L-L, Liu Y-J, Liu H-J, Qian T-T, Qi L-W, Wang X-R, Zeng Q-Y. 2014. Subcellular relocalization and positive selection play key roles in the retention of duplicate genes of *Populus* class III peroxidase family. *Plant Cell* **26**: 2404–2419.

Roignant J, Badel É, Leblanc-Fournier N, Brunel-Michac N, Ruelle J, Moulia B, Decourteix M. 2018. Feeling stretched or compressed? The multiple mechanosensitive responses of wood formation to bending. *Annals of Botany* **121**: 1151–1161.

Saidi I, Ammar S, Demont-CauletSaïda N, Thévenin J, Lapierre C, Bouzid S, Jouanin L. 2010. Thigmomorphogenesis in *Solanum lycopersicum*. *Plant Signaling & Behavior* **5**: 122–125.

Schneider CA, Rasband WS, Eliceiri KW. 2012. NIH Image to ImageJ: 25 years of image analysis. *Nature Methods* **9**: 671–675.

Schröder F, Lisso J, Lange P, Müssig C. 2009. The extracellular EXO protein mediates cell expansion in *Arabidopsis* leaves. *BMC Plant Biology* **9**: 20.

Scott TA, Melvin EH. 1953. Determination of dextran with anthrone. *Analytical Chemistry* **25**: 1656–1661.

Sehr EM, Agusti J, Lehner R, Farmer EE, Schwarz M, Greb T. 2010. Analysis of secondary growth in the *Arabidopsis* shoot reveals a positive role of jasmonate signalling in cambium formation. *The Plant Journal* **63**: 811–822.

Shannon P, Markiel A, Ozier O, Baliga NS, Wang JT, Ramage D, Amin N, Schwikowski B, Ideker T. 2003. Cytoscape: a software environment for integrated models of biomolecular interaction networks. *Genome Research* **13**: 2498–2504.

Šimura J, Antoniadi I, Široká J, Tarkowská D, Strnad M, Ljung K, Novák O. 2018. Plant hormonomics: multiple phytohormone profiling by targeted metabolomics. *Plant Physiology* **177**: 476–489.

Song D, Shen J, Li L. 2010. Characterization of cellulose synthase complexes in *Populus* xylem differentiation. *New Phytologist* **187**: 777–790.

de Souza A, Hull PA, Gille S, Pauly M. 2014. Identification and functional characterization of the distinct plant pectin esterases PAE8 and PAE9 and their deletion mutants. *Planta* **240**: 1123–1138.

Staswick PE, Tiryaki I. 2004. The oxylipin signal jasmonic acid is activated by an enzyme that conjugates it to isoleucine in *Arabidopsis*. *Plant Cell* **16**: 2117–2127.

Sundell D, Mannapperuma C, Netotea S, Delhomme N, Lin YC, Sjödin A, Van de Peer Y, Jansson S, Hvidsten TR, Street NR. 2015. The plant genome integrative explorer resource: PlantGenIE.org. *New Phytologist* **208**: 1149–1156.

Sundell D, Street NR, Kumar M, Mellerowicz EJ, Kucukoglu M, Johnsson C, Kumar V, Mannapperuma C, Delhomme N, Nilsson O *et al.* 2017. AspWood: high-spatial-resolution transcriptome profiles reveal uncharacterized modularity of wood formation in *Populus tremula*. *Plant Cell* **29**: 1585–1604.

Suzuki S, Li L, Sun Y-H, Chiang VL. 2006. The cellulose synthase gene superfamily and biochemical functions of xylem-specific cellulose synthase-like genes in *Populus trichocarpa*. *Plant Physiology* **142**: 1233–1245.

Takagi H, Ishiga Y, Watanabe S, Konishi T, Egusa M, Akiyoshi N, Matsuura T, Mori IC, Hirayama T, Kaminaka H *et al.* 2016. Allantoin, a stress-related purine metabolite, can activate jasmonate signaling in a MYC2-regulated and abscisic acid-dependent manner. *Journal of Experimental Botany* **67**: 2519–2532.

Taylor-Teeples M, Lin L, de Lucas M, Turco G, Toal TW, Gaudinier A, Young NF, Trabucco GM, Veling MT, Lamothe R *et al.* 2015. An *Arabidopsis* gene regulatory network for secondary cell wall synthesis. *Nature* **517**: 571–575.

Tejos R, Rodriguez-Furlán C, Adamowski M, Sauer M, Norambuena L, Friml J. 2018. PATELLINS are regulators of auxin-mediated PIN1 relocation and plant development in *Arabidopsis thaliana*. *Journal of Cell Science* **131**: jcs204198.

Telewski FW. 1989. Structure and function of flexure wood in *Abies fraseri*. *Tree Physiology* **5**: 113–121.

Telewski FW. 2016. Flexure wood: mechanical stress induced secondary xylem formation. In: Kim YS, Funada R, Singh AP, eds. *Secondary xylem biology.* Boston, MA, USA: Academic Press, 73–91.

Telewski FW. 2021. Mechanosensing and plant growth regulators elicited during the thigmomorphogenetic response. *Frontiers in Forests and Global Change* **3**: 574096.

Telewski FW, Jaffe MJ. 1986a. Thigmomorphogenesis: field and laboratory studies of *Abies fraseri* in response to wind or mechanical perturbation. *Physiologia Plantarum* **66**: 211–218.

Telewski FW, Jaffe MJ. 1986b. Thigmomorphogenesis: anatomical, morphological and mechanical analysis of genetically different sibs of *Pinus taeda* in response to mechanical perturbation. *Physiologia Plantarum* **66**: 219–226.

Telewski FW, Pruyn ML. 1998. Thigmomorphogenesis: a dose response to flexing in *Ulmus americana* seedlings. *Tree Physiology* **18**: 65–68.

Torres Acosta JA, de Almeida Engler J, Raes J, Magyar Z, De Groodt R, Inzé D, De Veylder L. 2004. Molecular characterization of *Arabidopsis* PHO80-like proteins, a novel class of CDKA;1-interacting cyclins. *Cellular and Molecular Life Sciences* **61**: 1485–1497.

Toyota M, Spencer D, Sawai-Toyota S, Jiaqi W, Zhang T, Koo AJ, Howe GA, Gilroy S. 2018. Glutamate triggers long-distance, calcium-based plant defense signaling. *Science* **361**: 1112–1115.

Updegraff DM. 1969. Semimicro determination of cellulose in biological materials. *Analytical Biochemistry* **32**: 420–424.

Urbanowicz BR, Peña MJ, Ratnaparkhe S, Avci U, Backe J, Steet HF, Foston M, Li H, O'Neill MA, Ragauskas AJ *et al.* 2012. 4-*O*-methylation of glucuronic acid in *Arabidopsis* glucuronoxylan is catalyzed by a domain of unknown function family 579 protein. *Proceedings of the National Academy of Sciences, USA* **109**: 14253–14258.

Van Moerkercke A, Duncan O, Zander M, Šimura J, Broda M, Bossche RV, Lewsey MG, Lama S, Singh KB, Ljung K *et al.* 2019. A MYC2/MYC3/

© 2023 The Authors
New Phytologist © 2023 New Phytologist Foundation

14698137, 0, Downloaded from https://nph.onlinelibrary.wiley.com/doi/10.1111/nph.19307 by Swedish University Of Agricultural Sciences, Wiley Online Library on [15/11/2023]. See the Terms and Conditions (https://onlinelibrary.wiley.com/terms-and-conditions) on Wiley Online Library for rules of use; OA articles are governed by the applicable Creative Commons License

MYC4-dependent transcription factor network regulates water spray-responsive gene expression and jasmonate levels. *Proceedings of the National Academy of Sciences, USA* **116**: 23345–23356.

Wang H, Jin Y, Wang C, Li B, Jiang C, Sun Z, Zhang Z, Kong F, Zhang H. 2017. Fasciclin-like arabinogalactan proteins, PtFLAs, play important roles in GA-mediated tension wood formation in *Populus*. *Scientific Reports* **7**: 6182.

Wang K, Yang Z, Qing D, Ren F, Liu S, Zheng Q, Liu J, Zhang W, Dai C, Wu M *et al.* 2018a. Quantitative and functional posttranslational modification proteomics reveals that TREPH1 plays a role in plant touch-delayed bolting. *Proceedings of the National Academy of Sciences, USA* **115**: E10265–E10274.

Wang Q, Qin G, Cao M, Chen R, He Y, Yang L, Zeng Z, Yu Y, Gu Y, Xing W *et al.* 2020a. A phosphorylation-based switch controls TAA1-mediated auxin biosynthesis in plants. *Nature Communications* **11**: 679.

Wang S, Yamaguchi M, Grienenberger E, Martone PT, Samuels AL, Mansfield SD. 2020b. The Class II KNOX genes KNAT3 and KNAT7 work cooperatively to influence deposition of secondary cell walls that provide mechanical support to *Arabidopsis* stems. *The Plant Journal* **101**: 293–309.

Wang Z, Winestrand S, Gillgren T, Jönsson LJ. 2018b. Chemical and structural factors influencing enzymatic saccharification of wood from aspen, birch and spruce. *Biomass and Bioenergy* **109**: 125–134.

Witasari LD, Huang F-C, Hoffmann T, Rozhon W, Fry SC, Schwab W. 2019. Higher expression of the strawberry xyloglucan endotransglucosylase/hydrolase genes FvXTH9 and FvXTH6 accelerates fruit ripening. *The Plant Journal* **100**: 1237–1253.

Wu T, Zhang P, Zhang L, Wang GG, Yu M. 2016. Morphological response of eight *Quercus* species to simulated wind load. *PLoS ONE* **11**: e0163613.

Xu P, Chen H, Hu J, Pang X, Jin J, Cai W. 2022. Pectin methylesterase gene *AtPMEPCRA* contributes to physiological adaptation to simulated and spaceflight microgravity in *Arabidopsis*. *iScience* **25**: 104331.

Xu W, Purugganan MM, Polisensky DH, Antosiewicz DM, Fry SC, Braam J. 1995. *Arabidopsis* TCH4, regulated by hormones and the environment, encodes a xyloglucan endotransglycosylase. *Plant Cell* **7**: 1555–1567.

Xu Y, Berkowitz O, Narsai R, De Clercq I, Hooi M, Bulone V, Van Breusegem F, Whelan J, Wang Y. 2019. Mitochondrial function modulates touch signalling in *Arabidopsis thaliana*. *The Plant Journal* **97**: 623–645.

Yan J, Huang Y, He H, Han T, Di P, Sechet J, Fang L, Liang Y, Scheller HV, Mortimer JC *et al.* 2019. Xyloglucan endotransglucosylase-hydrolase30 negatively affects salt tolerance in *Arabidopsis*. *Journal of Experimental Botany* **70**: 5495–5506.

Yang Z, Tian L, Latoszek-Green M, Brown D, Wu K. 2005. *Arabidopsis* ERF4 is a transcriptional repressor capable of modulating ethylene and abscisic acid responses. *Plant Molecular Biology* **58**: 585–596.

Yokoyama A, Yamashino T, Amano Y-I, Tajima Y, Imamura A, Sakakibara H, Mizuno T. 2007. Type-B ARR transcription factors, ARR10 and ARR12, are implicated in cytokinin-mediated regulation of protoxylem differentiation in roots of *Arabidopsis thaliana*. *Plant and Cell Physiology* **48**: 84–96.

Yuan Y, Teng Q, Zhong R, Ye Z-H. 2014. Identification and biochemical characterization of four wood-associated glucuronoxylan methyltransferases in *Populus*. *PLoS ONE* **9**: e87370.

Zang L, Zheng T, Chu Y, Ding C, Zhang W, Huang Q, Su X. 2015. Genome-wide analysis of the fasciclin-like arabinogalactan protein gene family reveals differential expression patterns, localization, and salt stress response in *Populus*. *Frontiers in Plant Science* **6**: 1140.

Zhang C, He M, Jiang Z, Liu L, Pu J, Zhang W, Wang S, Xu F. 2022. The xyloglucan endotransglucosylase/hydrolase gene *XTH22/TCH4* regulates plant growth by disrupting the cell wall homeostasis in *Arabidopsis* under boron deficiency. *International Journal of Molecular Sciences* **23**: 1250.

Zhang X, Dominguez PG, Kumar M, Bygdell J, Miroshnichenko S, Sundberg B, Wingsle G, Niittylä T. 2018. Cellulose synthase stoichiometry in aspen differs from *Arabidopsis* and Norway spruce. *Plant Physiology* **177**: 1096–1107.

Zhao Y, Wu G, Shi H, Tang D. 2019. RECEPTOR-LIKE KINASE 902 associates with and phosphorylates BRASSINOSTEROID-SIGNALING KINASE1 to regulate plant immunity. *Molecular Plant* **12**: 59–70.

Zhong R, Cui D, Ye Z-H. 2017. Regiospecific acetylation of xylan is mediated by a group of DUF231-containing *O*-acetyltransferases. *Plant and Cell Physiology* **58**: 2126–2138.

Zhong R, Cui D, Ye Z-H. 2018. A group of *Populus trichocarpa* DUF231 proteins exhibit differential *O*-acetyltransferase activities toward xylan. *PLoS ONE* **13**: e0194532.

Zhong R, Lee C, Zhou J, McCarthy RL, Ye ZH. 2008. A battery of transcription factors involved in the regulation of secondary cell wall biosynthesis in *Arabidopsis*. *Plant Cell* **20**: 2763–2782.

Zhong R, Ye Z-H. 2012. MYB46 and MYB83 bind to the SMRE sites and directly activate a suite of transcription factors and secondary wall biosynthetic genes. *Plant and Cell Physiology* **53**: 368–380.

Zhu XF, Wan JX, Sun Y, Shi YZ, Braam J, Li GX, Zheng SJ. 2014. Xyloglucan endotransglucosylase-hydrolase17 interacts with xyloglucan endotransglucosylase-hydrolase31 to confer xyloglucan endotransglucosylase action and affect aluminum sensitivity in *Arabidopsis*. *Plant Physiology* **165**: 1566–1574.

Zinkgraf M, Gerttula S, Zhao S, Filkov V, Groover A. 2018. Transcriptional and temporal response of *Populus* stems to gravi-stimulation. *Journal of Integrative Plant Biology* **60**: 578–590.

Supporting Information

Additional Supporting Information may be found online in the Supporting Information section at the end of the article.

Fig. S1 Effects of hybrid aspen (*Populus tremula* × *tremuloides*) stem flexing on tree growth kinetics.

Fig. S2 Effects of hybrid aspen (*Populus tremula* × *tremuloides*) stem flexing on sugar yield in enzymatic hydrolysates following acid pretreatment.

Fig. S3 Transcriptional changes in hybrid aspen (*Populus tremula* × *tremuloides*) trees in response to mechanical stimuli analyzed by GO enrichment.

Fig. S4 Phylogenetic tree of *CesA* gene family in *Arabidopsis thaliana*, *Populus trichocarpa* and *P. tremula*.

Fig. S5 Phylogenetic tree of *XTH* gene family in *Arabidopsis thaliana*, *Populus trichocarpa* and *P. tremula*.

Fig. S6 Phylogenetic tree of *ZAT* gene family in *Arabidopsis thaliana*, *Populus trichocarpa* and *P. tremula*.

Fig. S7 Phylogenetic tree of *TBL* gene family in *Arabidopsis thaliana*, *Populus trichocarpa* and *P. tremula*.

Methods S1 Detailed description of plant growing conditions, bioinformatic procedures, hormone analyses and statistical analyses.

Table S1 Hybrid aspen (*Populus tremula* × *tremuloides*) wood properties determined by SilviScan analysis at either 25 μm or 2 mm resolution.

Table S2 List of targeted compounds during general hormone profiling (shown also on Fig. 5).

Table S3 Differentially expressed genes ($P \leq 0.05$ and fold change (FC) ≥ 1.5) in the cambium tissue of flexed hybrid aspen

© 2023 The Authors
New Phytologist © 2023 New Phytologist Foundation

14698137, 0, Downloaded from https://nph.onlinelibrary.wiley.com/doi/10.1111/nph.19307 by Swedish University Of Agricultural Sciences, Wiley Online Library on [15/11/2023]. See the Terms and Conditions (https://onlinelibrary.wiley.com/terms-and-conditions) on Wiley Online Library for rules of use; OA articles are governed by the applicable Creative Commons License

(*Populus tremula* × *tremuloides*) stems relative to the stationary stems.

Table S4 Differentially expressed genes ($P \leq 0.05$ and fold change (FC) ≥ 1.5) in the xylem tissue of flexed hybrid aspen (*Populus tremula* × *tremuloides*) stems relative to the stationary stems.

Table S5 Gene Ontology enrichment analysis on the differentially expressed genes identified in the cambium tissue of flexed hybrid aspen (*Populus tremula* × *tremuloides*) stems relative to the stationary stems.

Table S6 List of transcription factors selected among the differentially expressed genes ($P \leq 0.05$ and fold change expression ≥1.5) in the cambium and xylem tissues of mechanically stimulated hybrid aspen (*Populus tremula* × *tremuloides*) stems compared with the stationary set.

Table S7 Gene Ontology Enrichment Analysis on the differentially expressed genes identified in the xylem tissue of flexed hybrid aspen (*Populus tremula* × *tremuloides*) stems relative to the stationary stems.

Table S8 List of genes from the co-expression clusters shown in Fig. 6(b).

Video S1 Representative hybrid aspen trees subjected to low-intensity stem flexures during their movement by the conveyor belt system in the phenotyping facility.

Please note: Wiley is not responsible for the content or functionality of any Supporting Information supplied by the authors. Any queries (other than missing material) should be directed to the *New Phytologist* Central Office.

© 2023 The Authors
New Phytologist © 2023 New Phytologist Foundation

14698137, 0, Downloaded from https://nph.onlinelibrary.wiley.com/doi/10.1111/nph.19307 by Swedish University Of Agricultural Sciences, Wiley Online Library on [15/11/2023]. See the Terms and Conditions (https://onlinelibrary.wiley.com/terms-and-conditions) on Wiley Online Library for rules of use; OA articles are governed by the applicable Creative Commons License